View metadata, citation and similar papers at core.ac.uk

brought to you by CORE

provided by Lehigh University: Lehigh Preserve

Lehigh University
Lehigh Preserve

Theses and Dissertations

1-1-1981

Estimated fatigue damage of the Blue Nile Bridge in Khartoum, Sudan.

Deborah J. Marcotte

Follow this and additional works at: http://preserve.lehigh.edu/etd

 Part of the Civil Engineering Commons

Recommended Citation

Marcotte, Deborah J., "Estimated fatigue damage of the Blue Nile Bridge in Khartoum, Sudan." (1981). *Theses and Dissertations.* Paper 1984.

This Thesis is brought to you for free and open access by Lehigh Preserve. It has been accepted for inclusion in Theses and Dissertations by an authorized administrator of Lehigh Preserve. For more information, please contact preserve@lehigh.edu.

ESTIMATED FATIGUE DAMAGE OF THE BLUE NILE BRIDGE IN KHARTOUM, SUDAN

by

Deborah J. Marcotte

A THESIS
Presented to the Graduate Committee
of Lehigh University
in Candidacy for the Degree of
Master of Science
in
Civil Engineering

Lehigh University
Bethlehem, Pennsylvania

November 1981

ProQuest Number: EP76257

All rights reserved

INFORMATION TO ALL USERS
The quality of this reproduction is dependent upon the quality of the copy submitted.

In the unlikely event that the author did not send a complete manuscript
and there are missing pages, these will be noted. Also, if material had to be removed,
a note will indicate the deletion.

ProQuest EP76257

Published by ProQuest LLC (2015). Copyright of the Dissertation is held by the Author.

All rights reserved.
This work is protected against unauthorized copying under Title 17, United States Code
Microform Edition © ProQuest LLC.

ProQuest LLC.
789 East Eisenhower Parkway
P.O. Box 1346
Ann Arbor, MI 48106 - 1346

CERTIFICATE OF APPROVAL

The thesis is accepted and approved in partial fulfillment of the requirements for the degree of Master of Science in Civil Engineering.

Nov. 24, 1981

Date

Dr. John W. Fisher

Dr. David A. VanHorn

ACKNOWLEDGMENTS

The research reported herein was conducted at Fritz Engineering Laboratory, Lehigh University, Bethlehem, Pennsylvania. The Director of Fritz Engineering Laboratory is Dr. Lynn S. Beedle, and the Chairman of the Department of Civil Engineering is Dr. David A. VanHorn.

The help and guidance of Dr. John W. Fisher, Project Director and Thesis Supervisor, is greatly appreciated. Special thanks are also due Dr. Ben T. Yen, Associate Project Director.

The staff at Fritz Engineering Laboratory is gratefully acknowledged for its assistance in the preparation of this report. Mr. Hugh T. Sutherland supervised the data acquisition, and Mrs. Ruth A. Grimes and Miss Shirley Matlock typed the manuscript.

Thanks are due the American Institute of Steel Construction and the United States Navy for their financial assistance to the author. The support and understanding of Mr. and Mrs. Alfred G. Marcotte, Mr. and Mrs. Matthaus A. Haist and Mr. Randall M. Haist is sincerely appreciated.

TABLE OF CONTENTS

LIST OF TABLES

LIST OF FIGURES

ABSTRACT

A field study of the Blue Nile Bridge in Khartoum, Sudan was undertaken by Lehigh University in the spring of 1981 to obtain measurements of transient strains in the structure due to present train traffic. The field data was then used in conjunction with data obtained from several theoretical models to estimate the accumulation of fatigue damage from operations to date, and to predict the useful fatigue life of critical components of the structure.

The stringers were noted to be the most critically stressed components of the Blue Nile Bridge, and the aforementioned analysis indicated that the stringers experienced stress cycles that exceeded the crack growth threshold and fatigue limit for both Category C and Category D of the AREA Specifications. Also, it was found that the effective stress range for the ten million random variable stress cycles that the stringers have experienced to date exceeded the lower confidence limit for Category C. Thus, it was concluded that detectable fatigue cracking has already occurred in one or more of the riveted stringer components and that the stringers of the Blue Nile Bridge should be retrofitted or replaced to prevent further fatigue damage.

In addition to the fatigue analysis of the Blue Nile Bridge described previously, all available references on past tests of riveted connections were reviewed, and the test data was compiled using cyclical loading type as a parameter. Each test was classified according to loading type as either a zero-to-tension test, a full reversal test or a half tension-to-tension test. The purpose of this investigation was to evaluate the effect of loading type on the fatigue behavior of riveted connections. It was concluded that Category C of the AREA Specification is a reasonable lower bound to fatigue resistance of riveted members and connections subjected to zero-to-tension or half tension-to-tension and with normal levels of rivet clamping force and bearing ratios of 2.25 or less. For all other riveted members and connections not meeting the above requirements, it was concluded that Category D is a reasonable lower bound to fatigue resistance, as per present AREA Specifications. It was also concluded that the compression portion of a full or partial reversal load cycle does not adversely affect the fatigue life of a riveted member or connection, and thus, should not be included in the calculation of the effective stress range.

1. INTRODUCTION

1.1 Background and Objectives

Railroad bridges are subjected to train loads (live loads) which cause stress variations (stress ranges) in various components. These stress ranges, in conjunction with the maximum stresses (caused by both live and dead loads) can affect the strength and integrity of bridges, particularly bridges which have been in service for a number of years. Therefore, when estimating the fatigue life or cumulative damage of an existing bridge, the stress range history due to live load and impact is of primary concern.

Field studies of several Sudan Railroad riveted truss bridges were undertaken by Lehigh University in the spring of 1981 to obtain measurements of the transient strains in each of the structures due to present train traffic. The field data was then used to estimate the accumulation of fatigue damage from operations to date, and to predict the useful life of critical components of the structures.

This report summarizes the field data and provides an analysis of the Blue Nile Bridge in Khartoum, Sudan.

The stress excursions at fourteen gage locations on various bridge components were monitored during the passage of typical train traffic for a two day period. A special work train, consisting of three diesel-electric locomotives, was also ordered for testing the stress response of the bridge. A summary of the field measurements

and a description of the data reduction method used is presented in this report.

A stress analysis was then made using six different analytical models of the main 65.53 m truss span, including several models of the floor system. The correlation between predicted stresses and measured stresses for all the gaged components, based on the work train test, is outlined later in this report.

A literature search of past tests on riveted connections was made in order to compile data to assess the feasibility of using Category C of the AREA Code as a reasonable lower bound to fatigue life estimations for some, if not all, riveted connections. This report includes a summary of the above data, and possible recommendations are also presented.

Finally, a fatigue damage assessment of the bridge was made based on assumed traffic to date, and an estimation was made of future traffic in order to predict if any fatigue failures would develop in the future. The results are found in the latter part of this report.

1.2 Description of Bridge

The Blue Nile Bridge carries the Sudan Government Railway across the Blue Nile River between Khartoum and Khartoum North (see Fig. 1). It has a total length between abutments of 558.93 m and for several years after its construction in 1909 was ranked as the longest and most important bridge in tropical Africa. In addition to the two

plate girder approach spans at the north and south banks, of length 12.19 m and 26.21 m, respectively, there are seven main riveted truss spans, each 66.60 m center-to-center of piers, and a rolling lift span at the northern end of the bridge giving a clear opening of 30.48 m. The bridge has a clear width between trusses of 10.97 m, which is divided into a 4.57 m clear width for railway traffic on the east side and a 6.40 m clear width for road traffic on the west side. There is also a cantilevered footpath, 3.53 m wide, carried outside the west trusses.

The main span trusses are of the Petit truss type and are 65.53 m in length between the centers of bearing. The floor beams are placed 3.66 m apart at panel points of the trusses. The railway track is carried by two lines of longitudinal stringers which are connected to the transverse floor beams. The roadway, which is supported on lontitudinal troughing with a span of 3.66 m, consists of concrete filling faced with asphalt. A plan and elevation of a typical main truss span are shown in Fig. 2, with a typical cross-section shown in Fig. 3.

The Blue Nile Bridge was constructed by the Cleveland Bridge and Engineering Company, Limited, of Darlington, England, from 1906 through 1909 and was opened to traffic in February 1909.

2. FIELD MEASUREMENTS

2.1 Data Acquisition

Field tests on the Blue Nile Bridge were conducted during a two day period in February 1981. The first main truss span at the southern end of the bridge was chosen for detailed investigation because of its accessibility. Fourteen strain gages were mounted on various components of this span to allow for the monitoring of transient strains caused by train traffic. Figure 4 shows schematically the approximate location of the fourteen strain gages. The exact position of all gages had to be estimated, as their locations were not well documented in the field.

All strain gages were 6 mm long electrical resistance foil gages and were compensated for temperature when connected.

The strain data was recorded only in analog form. The current in the gage was converted to a factored measure of the strain at the gage point in the bridge component by a Wheatstone Bridge circuit. Following amplification, the impulse was fed to an analog trace recorder. A flow diagram of the recording system is shown in Fig. 5.

The strain response of the bridge was recorded during the passage of regular train traffic for a two day period in order to obtain a statistically representative sample of traffic on the bridge. A total of four regular trains crossed the bridge during the field test (see Table 1). The resulting traffic sample was not considered

statistically significant and therefore was not used in further analysis.

A special work train was also ordered for testing the strain response of the bridge. The work train was made up of three diesel-electric locomotives (Engine Class 1800 to 1900). Figure 6 shows the work train consist. Crawl speed tests and higher speed tests were carried out using the work train consist in order to collect data for an accurate calculation of the impact factors of various bridge components. A maximum speed of 45 km/h was used during the field tests. Tests were also run in both directions (north and south) to assess the effect of train direction on the impact factors.

2.2 Data Reduction

Digital values of strains were not obtained during the field tests, therefore, manual measurement of the analog traces was the only possible method of data reduction. Some typical traces are shown in Fig. 7. By comparison of a trace of this type with the calibration data also recorded during the field tests, the magnitudes of the stress excursions were calculated. However, not all stress variations were considered stress cycles in the stress cycle counting method used in this analysis.

Prior to searching the analog traces for fatigue information, a logical stress or strain range counting procedure was defined. An initial threshold value was set at 1.0 mm for all traces. The

threshold value was the minimum strain (stress) range of interest. A cycle was defined by three successive extrema (two minima and a maximum or two maxima and a minimum), and the magnitude of the largest excursion between any two was defined as the range of the cycle. The third extremum of a cycle was used as the first extremum of the next cycle. For example, in Fig. 8, the points A, B, C, D, E, F, G, H, I and J are identified as extrema. Therefore, five ranges of magnitudes BC, CD, FG, GH and IJ are found. At the end of a signal, a special procedure was followed. Referring again to Fig. 8, only two of the three extrema for the final cycle (points I and J) are identified at the termination of the trace. The value IJ, however, is still classified as one stress range.

It was also noted that for a small threshold value, a large number of small ranges was found; whereas for a large threshold value, the procedure identified fewer, but larger, ranges. For example, again in Fig. 8, if the threshold value is initially assumed to be greater than EF, only four ranges of magnitudes BC, DG, GH and IJ are found.

Due to the fact that all ranges were specified as the absolute magnitudes of excursions, neither the absolute level of the trace, nor its polarity affected the end result of the data reduction.

2.3 Stresses in Various Components

Only the stress range data obtained from the nine passages of the work train consist was used in the analysis of the bridge. As stated previously, regular train traffic was infrequent and therefore not statistically significant. Also, an accurate train log of the regular train traffic was not kept. As a result, there was an insufficient amount of available data pertaining to the regular trains to warrant the use of these trains in further analysis.

It was noted, however, that each of the four regular trains observed was some type of passenger train. Thus, the data obtained from the passages of the regular trains was used as a purely qualitative comparative tool in the initial steps of the fatigue life estimation of critical members.

A computer program was developed to compile the strain range data obtained through data reduction of the analog traces. A subroutine was also developed to plot stress histograms for each gage (see Figs. 9 through 21). The maximum stress (S_{MAX}), the number of variable cycles (N_v), the root-mean-square stress range (S_{RRMS}) and Miner's stress range (S_{RMINER}) were also calculated for each gage within the main program. The results are presented in Table 2. Note that all the data compiled was obtained from field measurements of the work train consist.

2.4 Impact Considerations

Most specifications to date concur that impact on bridges, caused by vehicle loadings, is a function of the velocity of the vehicle. That is, as vehicle speed increases, the amount of impact created also increases. Therefore, the work train data was examined to extract a possible impact and vehicle velocity relationship for the Blue Nile Bridge.

The maximum speed attained in any of the work train passages was 45 km/h. The crawl speed test and the maximum velocity test were compared to note any variation in stresses or stress patterns caused by increased vehicle velocity. No variation was observed for any of the gaged members, including the stringers and floor beams. Thus, it was initially assumed that impact loading is negligible for the Blue Nile Bridge at present train speeds. However, the maximum velocity test was run at a relatively slow speed, and therefore, the test results should not have been used in the comparative analysis with the crawl run results. Hence, the final results of the impact analysis were actually inconclusive.

An investigation of the static and dynamic behavior of the Blue Nile Bridge, performed in 1960, noted that the dynamic deflection of the bridge exceeded the static deflection by less than 12%. The results of tests of both vertical and horizontal deflections were of a smaller order than expected. Thus, it was concluded that the Blue Nile Bridge was extremely steady under moving loads, and impact loading was not a major consideration (Coode and Partners, 1960). Therefore, impact loading was concluded to be negligible for the analysis presented herein.

3. THEORETICAL MODELS

3.1 Introduction to Analytical Models

A total of six finite element models were used to approximate the behavior of the 65.53 m through truss span of the Blue Nile Bridge (Bathe, et al., 1974). The six analytical models considered were as follows:

1. A plane simple truss model
2. A plane frame model
3. A three dimensional or space frame model
4. A simple beam model for the stringers
5. A continuous beam model for the stringers
6. A simple beam model for the floor beams

As a result of a field inspection of the Blue Nile Bridge in 1960, it was noted that most of the expansion bearings were performing as expected but were in need of regular cleaning and lubrication (Coode and Partners, 1960). Thus, all models were assumed to have fixed-roller bearings as the boundary conditions at support points. Also, it was noted during the field studies conducted by Lehigh University in February 1981 that corrosion was nonexistent due to the favorable inland climate of the Sudan. Therefore, the total gross section of all members was considered effective in each analytical model.

Each model was loaded in such a manner as to allow for the development of influence lines for stress resultants at any point in a specified member.

3.2 Plane Truss Model

A plane truss model is the analytical model most commonly used in the linear elastic analysis of a truss bridge span. It usually provides an upper bound to overall forces and displacements in the truss.

Figure 22 shows schematically the plane truss model used in the analysis of the Blue Nile Bridge. Table 3 lists the geometric properties of all truss elements. All truss joints were assumed to be pin connected. Simple floor beams were used to distribute loads to the trusses. Due to the unsymmetrical cross-section of the bridge, only the east truss was used in analysis, as it was the most critically stressed truss. A total of nine loading conditions was considered. Each loading condition consisted of a unit vertical load, multiplied by a factor of 1.555, applied at a lower chord panel point. Due to the symmetry of the plane truss model, only half the structure was loaded.

The plane truss model yielded only axial forces in the truss elements. Due to the fact that the loads on the bridge span are transmitted to hanger elements through the floor beams, the actual stress resultants in the hangers were approximated by also considering the hanger - floor beam frame action. Figure 23 shows the simplified hanger to floor beam frame model used in conjunction with the plane truss model. The hangers were assumed fixed at U_1, and the floor beam was assumed to be prismatic. The floor beam to hanger connection was considered continuous because of the relatively low flexural stiffness of the hanger as compared to that of the floor beam.

3.3 Plane Frame Model

A schematic of the plane frame model, identical to the plane truss model, is shown in Fig. 22. However, in the plane frame model, all joints were assumed to be rigidly connected. As a result of this assumption, moments developed at the ends of frame elements. Refer again to Table 3 for a listing of geometric properties of all elements.

The loading conditions were the same as used for the plane truss model. The hanger to floor beam frame model depicted in Fig. 23 was also used in conjunction with the plane frame model in order to more closely approximate the actual stresses in the hanger elements.

3.4 Space Frame Model

The three-dimensional or space frame model was developed to closely simulate the behavior of the full 65.53 m through truss span. The model included the floor system, both east and west trusses and the top and bottom lateral systems. Figure 24 shows schematically the three-dimensional model. The geometrical properties of the trusses are as listed for the plane truss and plane frame models in Table 3. The geometrical properties of the floor system members are summarized in Table 4.

The floor beam is a nonprismatic member, and thus, an average depth was used to estimate the corresponding geometrical properties. The portal cross-sectional properties were estimated, based on the assumption that each portal acts as a singular beam element and not a

truss or frame. It was noted that the top lateral system, including the portals, had no major interaction with the trusses or floor system except to provide a moment restraint at the upper ends of hanger elements.

In the three-dimensional model, floor beam to truss connections and stringer to floor beam connections were assumed to be rigid. All truss connections were also assumed to be rigid. That is, a plane frame model was used for each truss within the main space frame model.

The actual bridge structure is loaded directly on the rails. Thus, the three-dimensional model was loaded at quarter points and at midspan along both lines of longitudinal stringers. A total of 71 loading conditions was considered. Each loading condition consisted of two unit vertical loads applied at corresponding points on the two lines of longitudinal stringers. Torsional effects, although small, were also included.

3.5 Simple Beam Models

Both the stringers and floor beams were modeled as simple beams. The geometrical properties of both types of members are listed in Table 4.

Due to the fact that no interaction occurs between adjacent stringers in a simple beam model, only three loading conditions were considered for the stringer simple beam model. Each loading condition consisted of a unit vertical load applied at quarter points or at midspan of the model. Thus, the model simulated a typical stringer.

Only one loading condition was considered for the floor beam simple beam model, due to the fact that the floor beams are not connected directly to each other at any point in the structure. That is, in the simple beam model, any load applied to a floor beam had no effect on adjacent floor beams. Each floor beam was considered as a separate unit. The loading condition consisted of two unit vertical loads applied at stringer connection points of the floor beam model. Torsional effects were included.

3.6 Continuous Beam Model

The longitudinal lines of stringers were modeled as continuous beams on rigid supports, to note if the stringers act with any degree of continuity. Due to the symmetry of the continuous beam model, only 36 loading conditions were considered. Each loading condition consisted of a unit vertical load applied at quarter points or at midspan of the stringers.

3.7 Correlation of Predicted Stresses with Field Measurements

A problem arose in the correlation of predicted stresses with field measurements due to the fact that the gage locations were not well documented in the field. As a result, it was not possible to use all of the gages in the analysis reported herein. All gages located on the east truss members were used in the analysis, as their locations were approximately specified. However, the locations of gages 2, 11 and 12 were only arbitrarily documented and therefore were used with caution in the correlation of predicted and measured stresses.

A computer program was developed to calculate the maximum stresses, the root-mean-square stress ranges and Miner's stress ranges at specified points on members in a bridge structure subjected to moving loads. The three possible stress influence lines for each gage point, obtained from the analysis of the six theoretical models, were used in conjunction with the load pattern of the work train consist as input to the program described above. Also, stress-time plots were generated by the program to allow for a comparison with analog traces obtained in the field. Presented in Tables 5 through 10 is a summary of all data generated by the program. Figures 25 through 28 show typical stress-time plots (for gages 10 and 11) generated by the program. All data was based on the assumption that the gross section of the members is effective.

As a result of the correlation analysis, the space frame model was determined to be the most accurate model for the truss members. It was noted, however, that the maximum stresses measured at the gage locations in the bottom chords were slightly higher than those obtained from the theoretical analysis. In the three-dimensional model, it was assumed that movable bearings existed at one end of the bridge. Thus, it was concluded that the expansion bearings were allowing complete horizontal movement of the bridge. The three-dimensional model also overestimated the bending stresses in the top chord, as was expected. The maximum stresses and the stress ranges for all gage points on the east truss, obtained from the aforementioned computer analysis, varied slightly from those measured during

the field tests. A better correlation would have been possible if the exact locations of gages were known.

Normally, for a bridge of this type (through truss span), the floor beams and stringers behave as simple beams. However, the results presented herein led to a contradictory conclusion for the floor beams. It was noted that the simple beam model greatly overestimated the maximum stress and the stress ranges in the floor beams (see data corresponding to gage 10). The space frame model, on the other hand, provided excellent correlation with the field measurements for floor beams.

It was observed during the field tests that the stringers were subjected to stress excursions larger than expected at gage points 11 and 12. These critical gages were located at approximately the centers of adjacent stringers near the midspan of the bridge. Thus, it was expected that the simple beam model would provide an accurate correlation between predicted and measured stresses for the stringers. However, the maximum stresses predicted by the simple beam model, although larger than those stresses predicted by all other models, were at best, 43 percent less than the maximum stresses measured in the field. As a result, it was concluded that either the cross-sectional properties of the stringers, obtained from blue prints of the bridge and verified by a representative of the Sudan Government Railway, did not accurately represent actual field conditions, or the gage sensitivity was different than reported. Thus, it was suggested that additional field measurements of stringer dimensions were needed

MICRODEX CORRECTION GUIDE (M-8)

CORRECTION

The preceding document has been re-photographed to assure legibility and its image appears immediately hereafter.

RP 60000

REMINGTON RAND
OFFICE SYSTEMS DIVISION

the field tests. A better correlation would have been possible if the exact locations of gages were known.

Normally, for a bridge of this type (through truss span), the floor beams and stringers behave as simple beams. However, the results presented herein led to a contradictory conclusion for the floor beams. It was noted that the simple beam model greatly overestimated the maximum stress and the stress ranges in the floor beams (see data corresponding to gage 10). The space frame model, on the other hand, provided excellent correlation with the field measurements for floor beams.

It was observed during the field tests that the stringers were subjected to stress excursions larger than expected at gage points 11 and 12. These critical gages were located at approximately the centers of adjacent stringers near the midspan of the bridge. Thus, it was expected that the simple beam model would provide an accurate correlation between predicted and measured stresses for the stringers. However, the maximum stresses predicted by the simple beam model, although larger than those stresses predicted by all other models, were at best, 43 percent less than the maximum stresses measured in the field. As a result, it was concluded that either the cross-sectional properties of the stringers, obtained from blue prints of the bridge and verified by a representative of the Sudan Government Railway, did not accurately represent actual field conditions, or the gage sensitivity was different than reported. Thus, it was suggested that additional field measurements of stringer dimensions were needed

to provide a more accurate model for the stringers of the Blue Nile Bridge.

Due to the reversal in stress polarity at gages 2 and 4 (located on stringers near stringer to floor beam connections), it was also concluded that the stringers act with a small degree of joint continuity.

In conclusion, it was noted that the three-dimensional or space frame model provided the best correlation between measured and predicted stresses for both the truss members and the floor beams, whereas the simple beam model provided the closest correlation for the stringers. It should be noted, however, that an average correlation factor of 1.82 was used in conjunction with the simple beam model for stringers in all subsequent analyses. A comparison of Figs. 7 and 26 show the apparent discrepancy between predicted and measured stresses for the stringers. The validity of these conclusions is dependent on the data available at the time of the analysis.

4. RIVETED CONNECTIONS

4.1 Brief History

New technical developments in the 1850's led to more demanding use of rivets and riveted joints. However, investigations and research of the factors affecting riveted joint strength under both static and repeated loads were undertaken only after many failures of the new structures had occurred.

There are numerous references on riveted connections from approximately 1840 to date. In 1838, Fairbairn reported the results of an extensive series of static tests on riveted joints. Wilson and Thomas reported, in 1938, the results of fatigue tests on riveted joints in connection with the construction of the San Francisco - Oakland Bay Bridge, California. Later, in 1949, Lenzen discussed the results of an investigation limited to obtaining a comparison of the fatigue strength of riveted and bolted joints. The first major investigation on the effect of bearing pressure on the fatigue strength of riveted connections was performed by Parola, Chesson and Munse in 1965. Other researchers have studied the effect of grip length and rivet patterns on the fatigue strength of riveted connections (Parola, et al., 1965).

4.2 Present AREA Specifications

The present AREA Manual for Railway Engineering requires that all members with riveted connections that are subjected to fatigue or

repeated loadings must meet the requirements of Category D of Articles 1.3.13 and 2.3.1 in Chapter 15 of the specification. If an engineer can safely state that the rivets in question are tight and have developed a normal level of clamping force, Category C may be used as a lower bound for fatigue resistance estimations.

The current specification also establishes the definition for stress range (S_R) as the algebraic difference between the maximum (S_{MAX}) and minimum (S_{MIN}) calculated stresses. Thus, for members and connections subjected to reversal loadings, the compressive portion of the stress cycle is accounted for in the calculation of the stress range.

In Fig. 29, the Category D fatigue line of the AREA Specification is shown in comparison to fatigue resistance curves for riveted connections from the specifications of other countries.

4.3 Previous Investigation

As the result of a review of available test data, members with riveted connections had their lower bound fatigue resistance defined by the Category D fatigue line. The available test data was compiled using bearing ratio and level of clamping force as the only parameters. Figure 30 shows the results of this investigation. It was noted that most data pertaining to tests of riveted connections with reduced levels of clamping force fell to the right of the Category D fatigue line, but to the left of the Category C fatigue line. As a result, the lower bound to fatigue resistance of riveted connections was

defined as Category D in the AREA Specification. It was also noted that data pertaining to tests of riveted connections with reduced levels of clamping force, but with high bearing ratios, frequently fell to the left of the Category D fatigue line. However, these values were not considered applicable, as no railroad bridge structure had ever been proportioned using such high bearing ratios.

Figure 30 also shows that nearly all data associated with tests on riveted connections with normal levels of clamping force fell to the right of the design line corresponding to Category C. Therefore, it became permissible to use the Category C fatigue line when estimating the fatigue resistance of members with tight riveted joints. However, the decision as to what constitutes a tight riveted joint was left to the design engineer. Noted also was the fact that most data associated with tests of riveted connections with normal levels of clamping, but with high bearing ratios, fell to the left of the Category C fatigue line.

On the basis of this investigation into past test data of riveted connections, it was concluded that a decrease in fatigue life will generally accompany an increase in bearing ratio, especially when the bearing ratio is approximately 2.25 or greater. It was also concluded that fatigue life decereased with a decrease in the level of rivet clamping force. Thus, based on recommendations resulting from this study, the present AREA Specification was established (Fisher, et al., 1976).

4.4 Type of Stress Cycle and Fatigue Life

All available references on past tests of riveted connections were reviewed, and the test data was compiled using cyclical loading type as a parameter. Each test was classified according to loading type as either a zero-to-tension test, a full reversal test or a half tension-to-tension test. The purpose of this investigation was to evaluate the effect of loading type on the fatigue behavior of riveted connections. Thus, the effects caused by the variation of other parameters, such as rivet configuration, grip length and bearing ratio, were isolated from the effects produced by the variation of the parameter in question. However, the interaction of all variables was considered when interpreting the results reported herein.*

The test data obtained from all zero-to-tension tests are plotted in Fig. 31. Also plotted are the fatigue design lines corresponding to Category C and Category D of the AREA Specification. Most of the data which correspond to zero-to-tension fatigue tests fell to the right of the Category C design line. A small percentage of the test data fell between the two fatigue lines. These data points corresponded to zero-to-tension fatigue tests of riveted connections with a bearing ratio greater than 2.25, a reduced level of clamping force, or a combination of both factors.

Half tension-to-tension tests were performed infrequently in the past, and thus, only a small amount of data was available for the

---

*Table 11 summarizes the references and symbols used in Figs. 31 through 34.

purpose of this investigation (see Fig. 32). In general, the same results were obtained in the examination of half tension-to-tension tests as were previously described for zero-to-tension tests. It was also noted that half tension-to-tension loading resulted in yielding on the net section at the higher stress range levels. As stated previously, the AREA Specification defines stress range (S_R) as the algebraic difference between the minimum and maximum computed stresses. That is,

$$S_R = S_{MAX} - S_{MIN} \tag{1}$$

and thus, for half tension-to-tension load cycles,

$$S_{MAX} = 2\ S_R \tag{2}$$

Therefore, in the test data obtained, all values of stress range greater than or equal to approximately 110.32 MPa exceeded the yield stress on the net section for riveted connections of steel types A7 and A373. Thus, plastification and fatigue failure occurred simultaneously on the critical net sections of nearly all the riveted connections examined which were subjected to half tension-to-tension loading. As a result, an accurate estimate of the effect of half tension-to-tension loading on the fatigue life of riveted connections was not possible at higher levels of stress range.

Plotted in Fig. 33 are all the test data corresponding to the full reversal tests reviewed. In accordance with the AREA Specification, the stress ranges were calculated using Eq. 1. Thus, the compression half of each cycle was included in the comparative analysis.

It was noted that all data which corresponded to full reversal fatigue tests of riveted connections fell to the right of the Category C design line when the stress ranges were calculated as per AREA specifications. As a result of past research on riveted connections, it was generally concluded that reversal loading reduces the fatigue strength and endurance limit of the connection in question. Thus, it was proposed during this investigation that the definition of stress range as per the present AREA Specification was not conservative for members and connections subjected to full or partial reversal loadings.

The stress ranges corresponding to the full reversal tests were recalculated according to the following assumptions:

$$S_{MIN} = 0 \tag{3}$$

and

$$S_R = S_{MAX} \tag{4}$$

Note that only the tensile portion of the full cycle was used in determining the magnitude of the stress range on the net section of the specimen. The compression half of the cycle does not adversely affect the fatigue life of a riveted connection. A comparison of the adjusted test data and the AREA fatigue lines (see Fig. 34) shows that nearly all the test data fell between the Category C line and the Category D line. Thus, a conservative lower bound to fatigue resistance of riveted connections subjected to reversal loading was noted as the Category D fatigue line.

The variation of fatigue strength with bearing pressure was observed to be small for a riveted connection subject to full reversal loading. Also, no data from full reversal tests with reduced rivet clamping was obtained due to the difficulty inherent in performing a test of this nature.

The feasibility of increasing the fatigue or endurance limit for riveted connections was also investigated. Figures 31 and 32 show that the present endurance limit of 68.95 MPa for Category C was conservative for zero-to-tension and half tenstion-to-tension tests. No test data was obtained at the endurance limit of Category C or Category D from the full reversal tests reviewed. It was also noted that no experimental data exists at a cycle life greater than 10^7. Hence, the fatigue limit and crack growth threshold are not well defined for riveted members and connections.

4.5 Summary and Recommendations

On the basis of the test results referred to herein, several general observations were made concerning the effect of different variables on the fatigue life of riveted connections. A reduction in the amount of rivet clamping decreased the fatigue life of riveted connections, regardless of the type of load cycle. The variation of fatigue strength with bearing ratio was small for riveted connections subjected to full reversal loading. However, for zero-to-tension and half tension-to-tension loadings, the variation was much greater and appeared to be most pronounced when the bearing ratio was 2.25 or

greater. Fatigue properties increased with an increase in grip length for the zero-to-tension loading, but decreased for the full reversal loading. In general, the full reversal loading was observed to be the most critical type of loading investigated.

It was noted that all data corresponding to fatigue tests of beams with riveted cover plates fell well to the right of the Category C design line. However, only zero-to-tension tests were performed on this type of specimen. Also, simple riveted tension splice test data always fell to the right of the Category C fatigue line for specimens subjected to zero-to-tension or half tension-to-tension loading. It should be noted, however, that both the simple tension splice specimens and the beams with cover plates had normal levels of rivet clamping force and bearing ratios of 2.25 or less. Thus, for the restrictions mentioned above, it was concluded that Category C is a reasonable lower bound to fatigue resistance of riveted members and connections subjected to zero-to-tension or half tension-to-tension load cycles.

The following tentative recommendations for possible changes in the AREA Specification were based on the results of the investigation reported herein.

1. Members with riveted connections subjected to zero-to-tension or partial tension-to-tension load cycles shall meet the requirements of Category C of the AREA Specification, except as noted below.

2. Members with riveted connections subjected to zero-to-tension or partial tension-to-tension load cycles and with severely reduced levels of clamping force shall meet the requirements of Category D of the AREA Specification.

3. For members with riveted connections subjected to full or partial reversal load cycles, the effective stress range shall be defined as the maximum calculated net section stress.

4. Members with riveted connections subjected to full or partial reversal load cycles shall, in all cases, meet the requirements of Category D of the AREA Specification.

It should be noted that the above recommendations were based on the assumption that the allowable bearing ratio was 2.25 or less.

5. FATIGUE DAMAGE ESTIMATES

5.1 History of Traffic on the Bridge

In order to determine the remaining life of the Blue Nile Bridge, an estimate of past and future train traffic on the bridge was made (see Fig. 35). Table 12 summarizes the number of trains per year estimated from tertiary sources. The following assumptions were also made:

1. From 1909 to 1935, only steam locomotives of the type 200 were used.
2. From 1935 to 1960, only steam locomotives of the type 500 were used.
3. From 1960 to date, diesel-electric locomotives were used. The 1800 locomotive was most common.
4. Passenger trains had a maximum of 25 cars per train from 1909 to the present.
5. Freight trains had a maximum of 35 cars per train from 1909 to 1960. No oil freight was shipped before 1960.
6. Freight trains had a maximum of 50 cars per train from 1960 to date, with approximately 40 percent of the cars as oil freight cars.
7. Approximately half of the total number of oil freight cars transported during the time period 1960 to date were empty.

8. Unit trains consisted of a diesel-electric locomotive, type 1800, and four passenger cars.

9. Freight cars were full at all times, in both directions.

Table 13 summarizes the number of locomotives and cars calculated using the aforementioned assumptions.

It was noted in the 1960 field study of the Blue Nile Bridge that train loading created critical stresses in the stringers independently of truck loading on the roadway. It was also observed that truck loadings, acting independently of train loadings did not adversely affect the stringers. It was also noted in this study that the floor beams were adversely affected by truck traffic. However, the cumulative fatigue damage on the floor beams due to truck traffic was minor in comparison to that caused by train traffic. Also, due to the recent industrial development in Khartoum North, a separate road bridge was built over the Blue Nile between Khartoum and Khartoum North, and the Blue Nile Bridge was closed to truck traffic. As a result of the above findings, truck traffic was not considered critical in the estimation of fatigue damage of the bridge, and thus, was not included in any subsequent calculations.

5.2 Estimation of Fatigue Life of Critical Members

The stringers were noted to be the most critically stressed members. Also considered relatively critical were the hangers and floor beams. The three-dimensional model was used to simulate the behavior

of the hangers and floor beams, whereas the simple beam model was used to represent the stringers. Correlation factors used in conjunction with these models are summarized in Table 14. The most critical points on the three types of critical members were chosen for further analysis, as follows:

1. Rivet holes in first hanger at floor beam to hanger connection
2. Rivet holes at midspan of stringer.
3. Rivet holes in center floor beam at floor beam to stringer connection.

The net section was assumed effective in all cases.

The program developed to assist in analyzing the various theoretical models was also used to estimate S_{RRMS} and S_{RMINER} for each critical member at the point designated above on the basis of present and future traffic estimations. The results are presented in Tables 15 through 17.

The fatigue life estimations for the three critical members are presented in Table 18 and Figs. 36 through 38. It is noted that the hangers and floor beams are not expected to experience fatigue cracks. However, the strain measurements obtained from the field study indicated that the stringers experienced stress cycles that exceeded the crack growth threshold and fatigue limit for both Category C and Category D of the AREA Specifications. The effective stress range for the ten million random variable stress cycles that the stringers have

experienced to date indicates that fatigue cracks are likely to develop in the stringers. The effective stress range and cumulative stress cycles for the stringers to date exceeds the lower confidence limit for Category C of the AREA Specifications. Thus, it was concluded that cracks should become apparent in one or more of the riveted stringer components. These cracks should be readily detectable as the material properties of the steel indicate that brittle fractures are not likely to occur unless the riveted component (i.e. flange angle) has been severed by fatigue cracking. Because of the inherent redundancy of the multiple component stringers, cracking of one of the components will not result in significant deformation or loss of ability to carry the load. Frequent inspections should permit the immediate detection of such fatigue cracks, so that satisfactory retrofitting can be carried out.

Due to the fact that the fatigue damage, to date, of the stringers has been estimated as critical, it was concluded that steps need to be taken in order to strengthen or replace the stringers of the Blue Nile Bridge.

5.3 Conclusions

The following conclusions are based on the analysis and assumptions presented herein.

1. The three-dimensional model provided the best correlation between measured and predicted stresses for the floor

beams and hangers, whereas the simple beam model provided the best correlation for the stringers.

2. Field measurement of the dimensions of the stringers is recommended, as there were major discrepancies between actual and theoretical stresses. That is, the measured stresses were much larger than those obtained from the theoretical analysis.

3. The floor beams and hangers were found to have adequate resistance to fatigue loading and no crack growth is anticipated.

4. The stringers were found to have already developed detectable fatigue cracking. It was concluded that a more accurate estimate of the past train traffic is needed in order to obtain a better approximation of fatigue life for the stringers. However, it was also concluded that the stringers must be retrofitted or replaced to prevent further fatigue damage, as they appeared to be critically stressed.

5. The results presented herein suggest that a serious effort must be made to inspect the stringers in order to ascertain whether or not cracks have formed.

TABLE 1: REGULAR TRAIN TRAFFIC RECORDED

DURING FIELD TEST PERIOD

Date	Time	Train Description
2-15-81	0715	Northbound Passenger Train with Four Freight Cars
2-15-81	0735	Northbound Passenger Train
2-15-81	0758	Three Lightweight Self-Propelled Northbound Passenger Cars
2-15-81	0915	Northbound Passenger Train

TABLE 2: STRESSES AT GAGE POINTS IN VARIOUS COMPONENTS DUE TO WORK TRAIN

Gage No.	Gage Position	S_{MAX} (MPa)	S_{RRMS} (MPa)	S_{RMINER} (MPa)	N_v
1	Bottom Chord	23.79	16.48	17.24	17
2	Stringer	23.80	14.89	15.93	139
3	Bottom Chord	21.99	13.86	14.75	24
4	Stringer	21.97	17.80	19.10	92
5	Rail	91.52	72.74	74.67	155
6	Hanger	38.27	16.13	17.31	40
7	Diagonal	12.82	10.14	10.48	41
8	Hanger	25.63	16.82	18.55	45
9	Diagonal	23.80	16.82	18.06	37
10	Floor Beam	20.14	13.31	13.86	51
11	Stringer	78.71	71.98	72.05	48
12	Stringer	84.20	73.64	73.77	48
13	Floor Beam	No Cycles Discernable			
14	Top Chord	16.47	17.58	17.72	8

TABLE 3: CROSS-SECTIONAL PROPERTIES OF TRUSS MEMBERS (GROSS SECTION)

Member	Area (cm^2)	Moment of Inertia (cm^4)	
		I_x	I_y
L0-L4	645.22	616210.65	544525.61
L4-L8	914.58	932039.98	800571.62
L8-L9	979.09	987532.78	867124.94
L0-M1	899.74	1538156.60	480016.81
M1-U2	823.55	1396021.90	461947.79
U2-U4	798.45	981335.10	736783.32
U4-U6	769.42	945614.53	716554.47
U6-U10	895.55	1067647.30	803898.97
L1-M1	114.13	44854.35	1047.65
L3-M3	114.13	44854.35	1047.65
L5-M5	114.13	44854.35	1047.65
L7-M7	114.13	44854.35	1047.65
L9-M9	114.13	44854.35	1047.65
L2-U2	151.61	58391.03	1474.29
L6-U6	151.61	58391.03	1474.29
L4-U4	118.52	45625.21	1030.59
L8-U8	128.32	57476.57	4777.50
L2-M1	114.13	50159.22	2869.92
L2-M3	114.13	50159.22	2869.92
L4-U2	271.03	134769.49	29514.55
L4-U6	278.19	133946.60	66363.52
L6-M5	123.94	56274.78	4808.31
L6-M7	123.94	56274.78	4808.31
L8-M9	123.94	56274.78	4808.31
L8-U6	215.61	99819.79	12960.20
U8-M9	109.29	47154.44	2123.61
M8-M9	75.87	4982.29	39825.44

TABLE 4: CROSS-SECTIONAL PROPERTIES OF FLOOR SYSTEM MEMBERS (GROSS SECTION)

Member	Area (cm^2)	Moment of Intertia (cm^4) I_x	I_y
Floor Beam	349.61	997678.42	10473.63
Stringer	125.10	50380.65	2254.31

TABLE 5: MAXIMUM STRESSES IN TRUSS MEMBERS OF THEORETICAL MODELS DUE TO WORK TRAIN CONSIST

Gage	Position	Maximum Stresses (MPa)			
		Measured	Plane Truss	Plane Frame	Space Frame
1	Bottom Chord	23.79	19.84	22.94	22.09
3	Bottom Chord	21.99	19.84	21.12	20.53
6	Hanger	38.27	30.72	15.86	24.67
7	Diagonal	12.82	30.56	16.51	14.86
8	Hanger	25.63	28.35	19.52	24.14
9	Diagonal	23.80	37.74	20.48	21.13
14	Top Chord	-16.47	-20.81	-21.65	-19.04

TABLE 6: MAXIMUM STRESSES IN FLOOR SYSTEM MEMBERS OF THEORETICAL MODELS DUE TO WORK TRAIN CONSIST

Gage	Position	Maximum Stresses (MPa) Measured	Simple Beam	Space Frame	Continuous Beam
2*	Stringer	23.79 -16.47	13.52	-23.52	-20.55
4*	Stringer	-21.97 14.64	-18.31	21.57	-14.22
10	Floor Beam	20.14	34.86	20.48	---
11	Stringer	78.71	44.65	30.90	30.70
12	Stringer	84.20	44.65	31.21	30.7-

*Traces showed change in sign of stress as trains passed

TABLE 7: ROOT-MEAN-SQUARE STRESS RANGES IN TRUSS MEMBERS OF THEORETICAL MODELS DUE TO WORK TRAIN CONSIST

Gage	Position	Measured	Stress Ranges (MPa) Plane Truss	Plane Frame	Space Frame
1	Bottom Chord	16.48	19.84	22.94	17.56
3	Bottom Chord	13.86	19.84	21.12	14.21
6	Hanger	16.13	14.89	9.66	13.97
7	Diagonal	10.14	12.94	9.45	11.32
8	Hanger	16.82	17.35	11.82	16.75
9	Diagonal	16.82	16.03	15.62	16.03
14	Top Chord	17.58	20.81	21.65	19.04

TABLE 8: ROOT-MEAN-SQUARE STRESS RANGES IN FLOOR SYSTEM MEMBERS OF THEORETICAL MODELS DUE TO WORK TRAIN CONSIST

Gage	Position	Stress Ranges (MPa)			
		Measured	Simple Beam	Space Frame	Continuous Beam
2	Stringer	14.89	8.12	16.07	17.69
4	Stringer	17.80	10.96	17.57	10.98
10	Floor Beam	13.31	29.82	13.28	---
11	Stringer	71.98	38.98	28.33	28.10
12	Stringer	73.64	38.98	29.01	28.10

TABLE 9: MINER'S STRESS RANGES IN TRUSS MEMBERS OF THEORETICAL MODELS DUE TO WORK TRAIN CONSIST

Gage	Position	Stress Ranges (MPa) Measured	Plane Truss	Plane Frame	Space Frame
1	Bottom Chord	17.24	19.84	22.94	18.03
3	Bottom Chord	14.75	19.84	21.12	15.98
6	Hanger	17.31	15.77	11.71	15.86
7	Diagonal	10.48	16.29	11.58	12.01
8	Hanger	18.55	19.08	13.95	18.47
9	Diagonal	18.06	18.33	17.38	17.65
14	Top Chord	17.72	20.81	21.65	19.04

TABLE 10: MINER'S STRESS RANGES IN FLOOR SYSTEM MEMBERS OF THEORETICAL MODELS DUE TO WORK TRAIN CONSIST

			Stress Ranges (MPa)		
Gage	Position	Measured	Simple Beam	Space Frame	Continuous Beam
2	Stringer	15.93	9.31	17.32	18.21
4	Stringer	19.10	12.44	18.67	12.71
10	Floor Beam	13.86	30.26	13.90	---
11	Stringer	72.05	40.29	29.20	28.98
12	Stringer	73.77	40.29	30.30	28.98

TABLE 11: REFERENCE LIST FOR RIVETED CONNECTION

LITERATURE SEARCH

Symbol	Condition	References
△	I Beams with Riveted Cover Plates	6
○	Single and Double Lap Riveted Joints	3, 4, 9, 17
⧓	Double Lap Joint Bearing Ratio < 2.25 Reduced Clamping	14, 17
■	Double Lap Joint Bearing Ratio < 2.25 Normal Clamping	14, 17
⧗	Double Lap Joint Bearing Ratio > 2.25 Reduced Clamping	14, 17
●	Double Lap Joint Bearing Ratio > 2.25 Normal Clamping	14, 17

TABLE 12: NUMBER OF TRAINS PER YEAR

ESTIMATED FROM TERTIARY SOURCES

Year	Freight Trains	Passenger Trains	Unit Trains*
1909	1440	648	0
1935	1440	648	0
1960	1440	648	0
1981	5280	1176	312
2000 (high)	8754	1654	594
2000 (low)	5280	1176	312

*Small passenger trains with three or four passenger cars

TABLE 13: NUMBER OF LOCOMOTIVES AND CARS ESTIMATED FROM TERTIARY SOURCES

Car Type	Year 1981	2000 (Low Estimate)	2000 (High Estimate)
200 Locomotive	54,288	54,288	54,288
500 Locomotive	52,200	52,200	52,200
1800 Locomotive	97,416	226,008	268,351
Freight Car	4,788,000	7,797,600	8,839,890
Oil Freight Car (Full)	739,200	1,742,400	2,089,830
Oil Freight Car (Empty)	739,200	1,742,400	2,089,830
Passenger Car	1,341,528	1,923,840	2,054,557
	7,072,632	13,538,736	15,448,946

TABLE 14: CORRELATION FACTORS

Member Type	Correlation Factors (Actual/Predicted) Maximum Stress	S_{RRMS}	S_{RMINER}
Hanger	1.30	1.08	1.05
Floor Beam	0.98	1.00	1.00
Stringer	1.82	1.87	1.81

TABLE 15: EFFECTIVE STRESS RANGE ESTIMATES

DUE TO CUMULATIVE TRAFFIC TO DATE

1981 ($N_v = 9.98 \times 10^6$)

Member Type	S_{RRMS} (MPa)	S_{RMINER} (MPa)	S_{RMAX} (MPa)
Floor Beam	8.704	10.138	29.43
Stringer	47.505	48.477	85.27
Hanger	14.575	15.412	47.02

TABLE 16: EFFECTIVE STRESS RANGES, ASSUMING NO INCREASE IN VOLUME OF TRAIN TRAFFIC PER YEAR (LOW ESTIMATE) FOR CUMULATIVE TRAFFIC TO 2000

	2000 ($N_v = 1.69 \times 10^7$)		
Member Type	S_{RRMS} (MPa)	S_{RMINER} (MPa)	S_{RMAX} (MPa)
Floor Beam	8.837	10.190	29.43
Stringer	47.591	48.495	85.27
Hanger	14.777	15.563	47.02

TABLE 17: EFFECTIVE STRESS RANGES ASSUMING A CONTINUATION IN THE PRESENT GROWTH OF THE VOLUME OF TRAIN TRAFFIC PER YEAR (HIGH ESTIMATE) FOR CUMULATIVE TRAFFIC TO 2000

2000 ($N_v = 1.92 \times 10^7$)

Member Type	S_{RRMS} (MPa)	S_{RMINER} (MPa)	S_{RMAX} (MPa)
Floor Beam	8.868	9.990	29.43
Stringer	47.663	48.723	85.27
Hanger	14.852	15.619	47.02

TABLE 18: FATIGUE LIFE ESTIMATIONS OF CRITICAL MEMBERS

	Category C		Category D	
	S_{RRMS}	S_{RMINER}	S_{RRMS}	S_{RMINER}
Floor Beam	Infinite Life		Infinite Life	
Hanger	Infinite Life		Infinite Life	
Stringer (High Estimate)	High Probability of Cracking*		High Probability of Cracking*	
Stringer (Low Estimate)	High Probability of Cracking*		High Probability of Cracking*	

*The lower confidence limit for the category in question has already been reached.

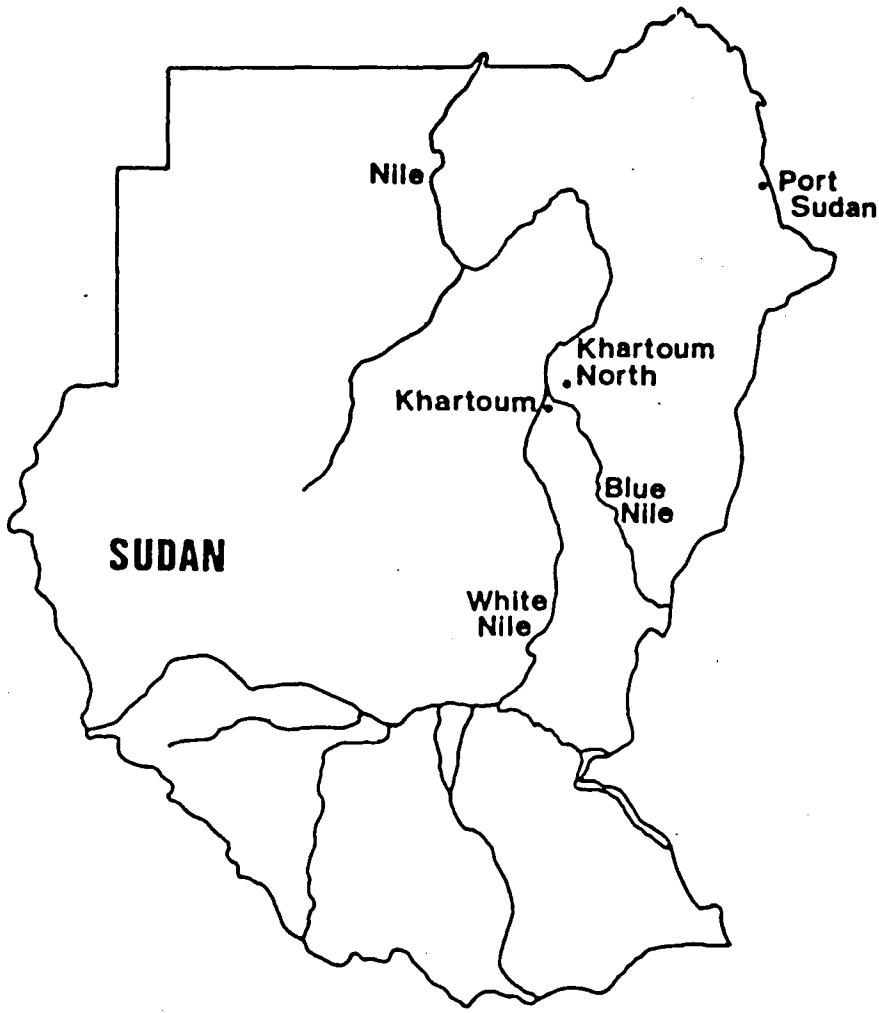

Fig. 1 Geographic Location of Blue Nile Bridge

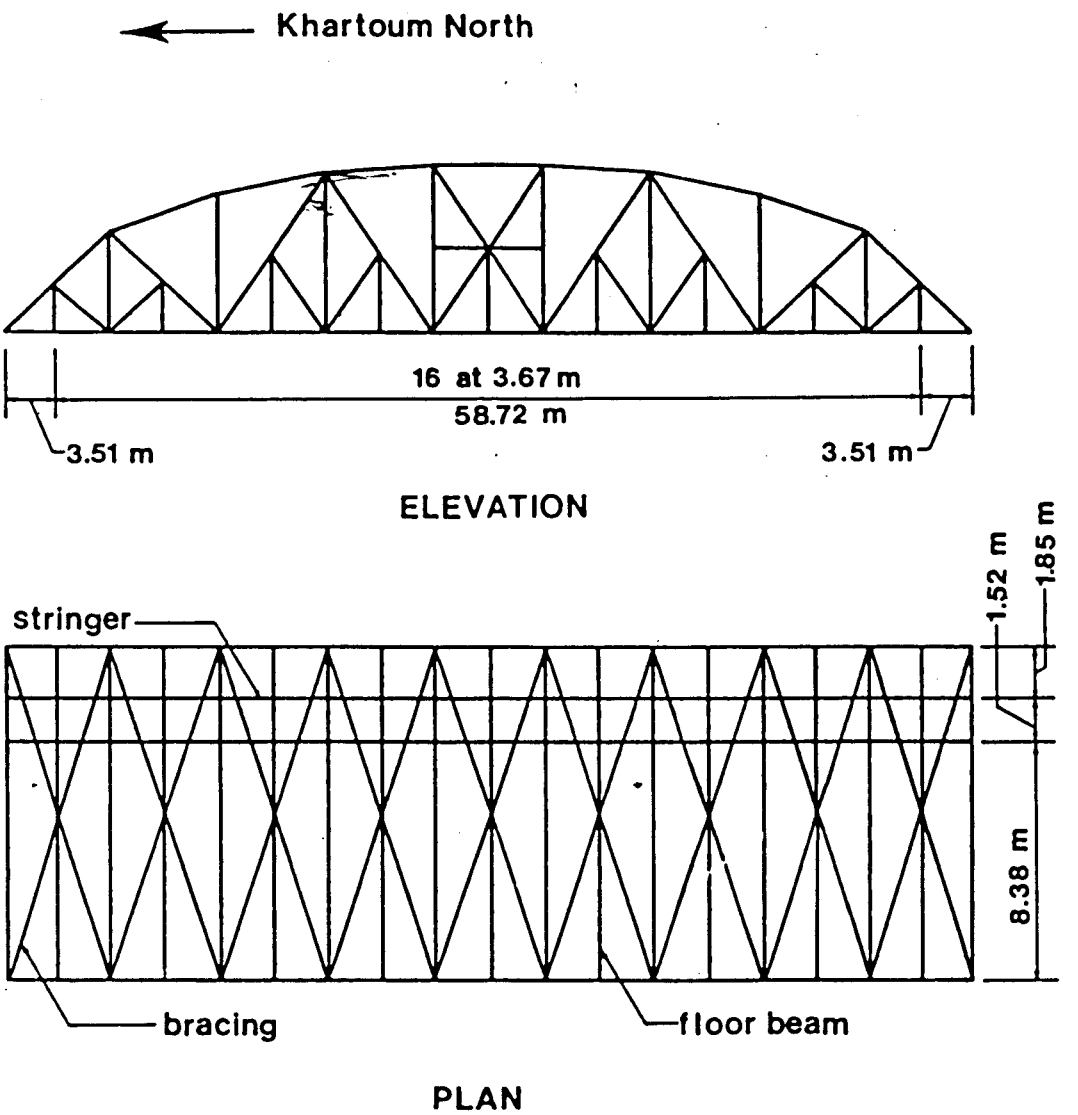

Fig. 2 Plan and Elevation of Typical Main Truss Span

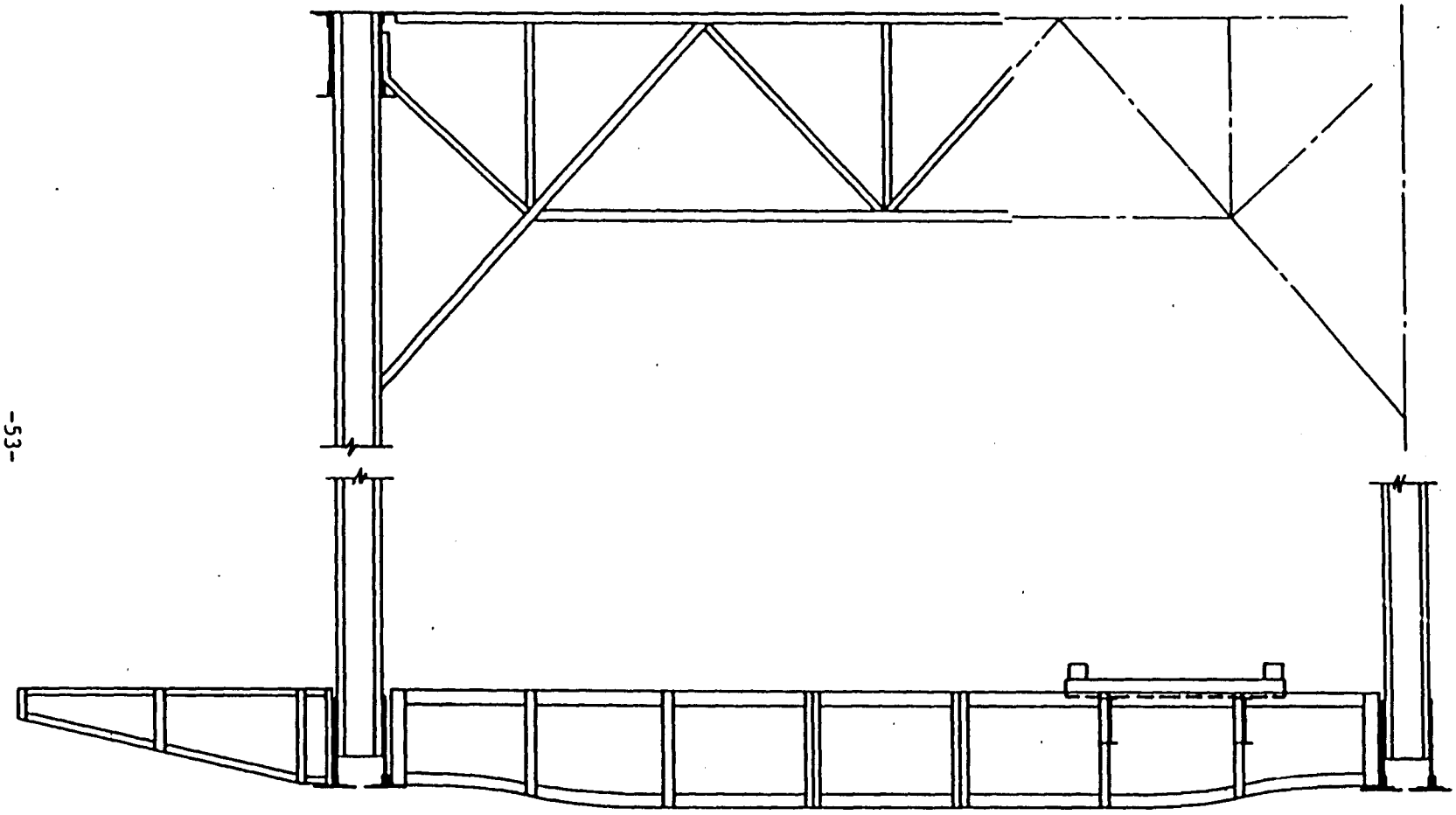

Fig. 3 Cross-Section of Typical Main Truss Span

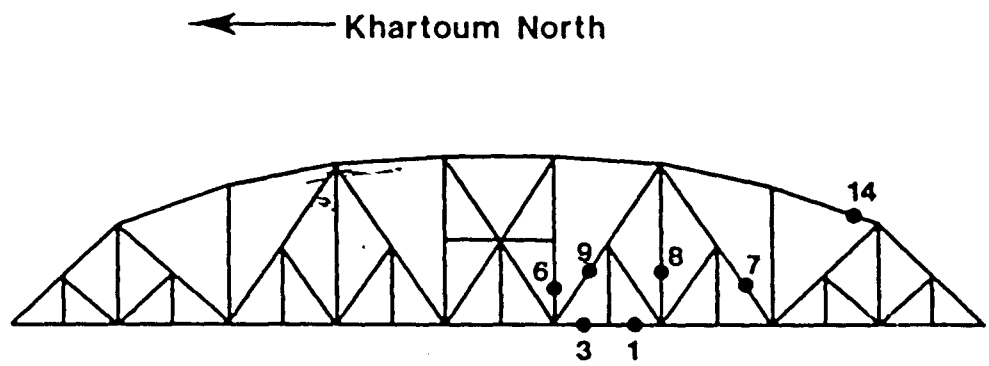

EAST TRUSS

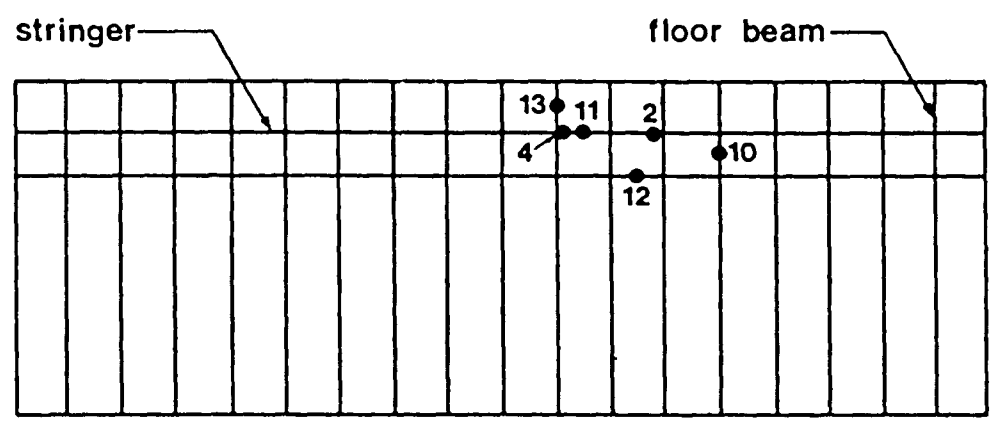

FLOOR SYSTEM

Fig. 4 Approximate Location of Strain Gages

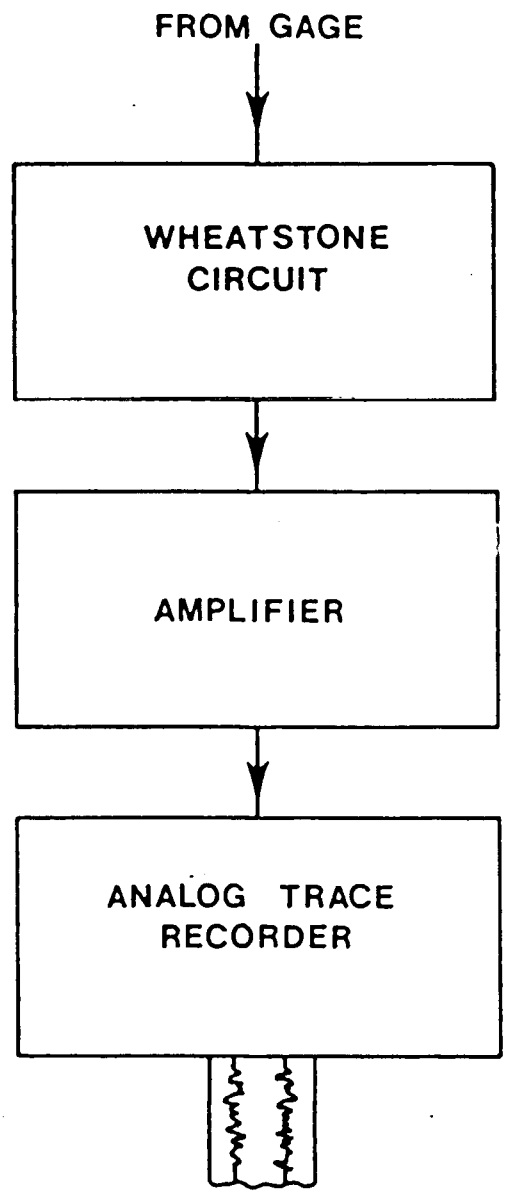

Fig. 5 Flow Diagram of Recording System

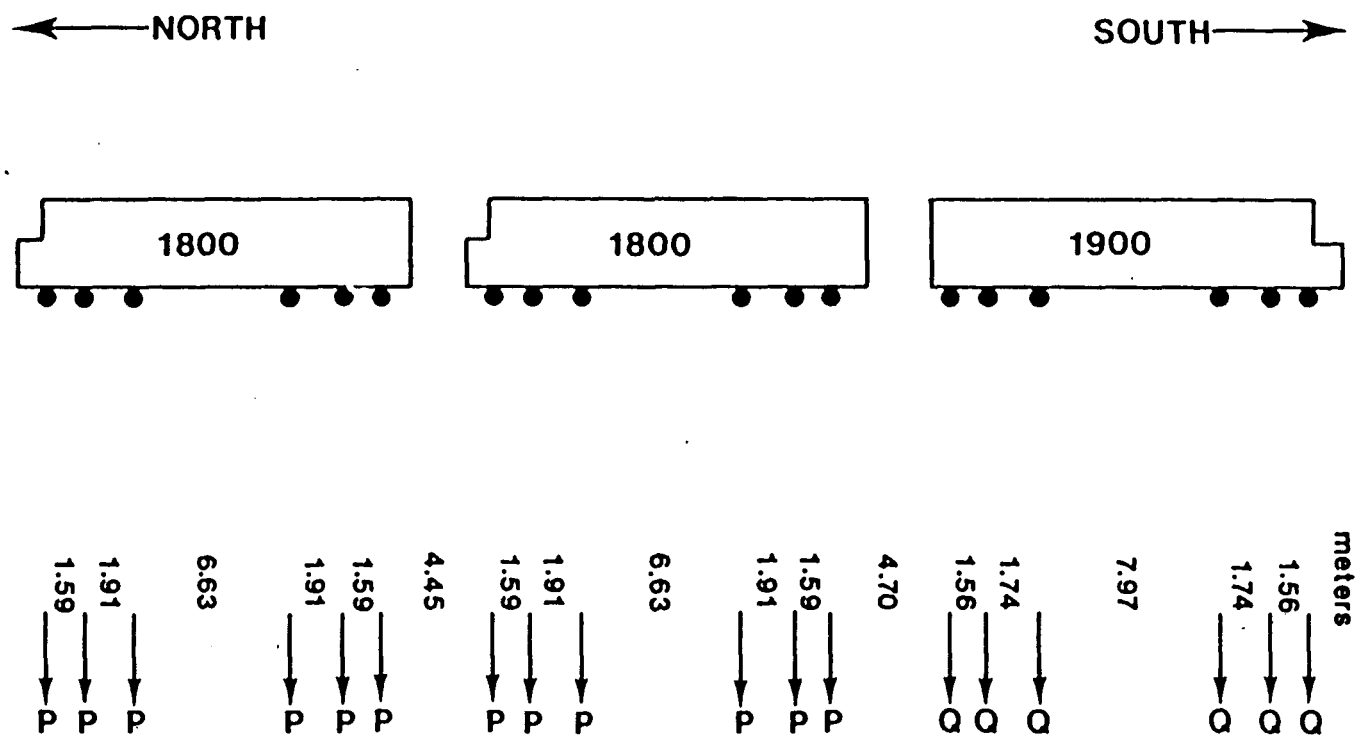

Fig. 6 Work Train Consist

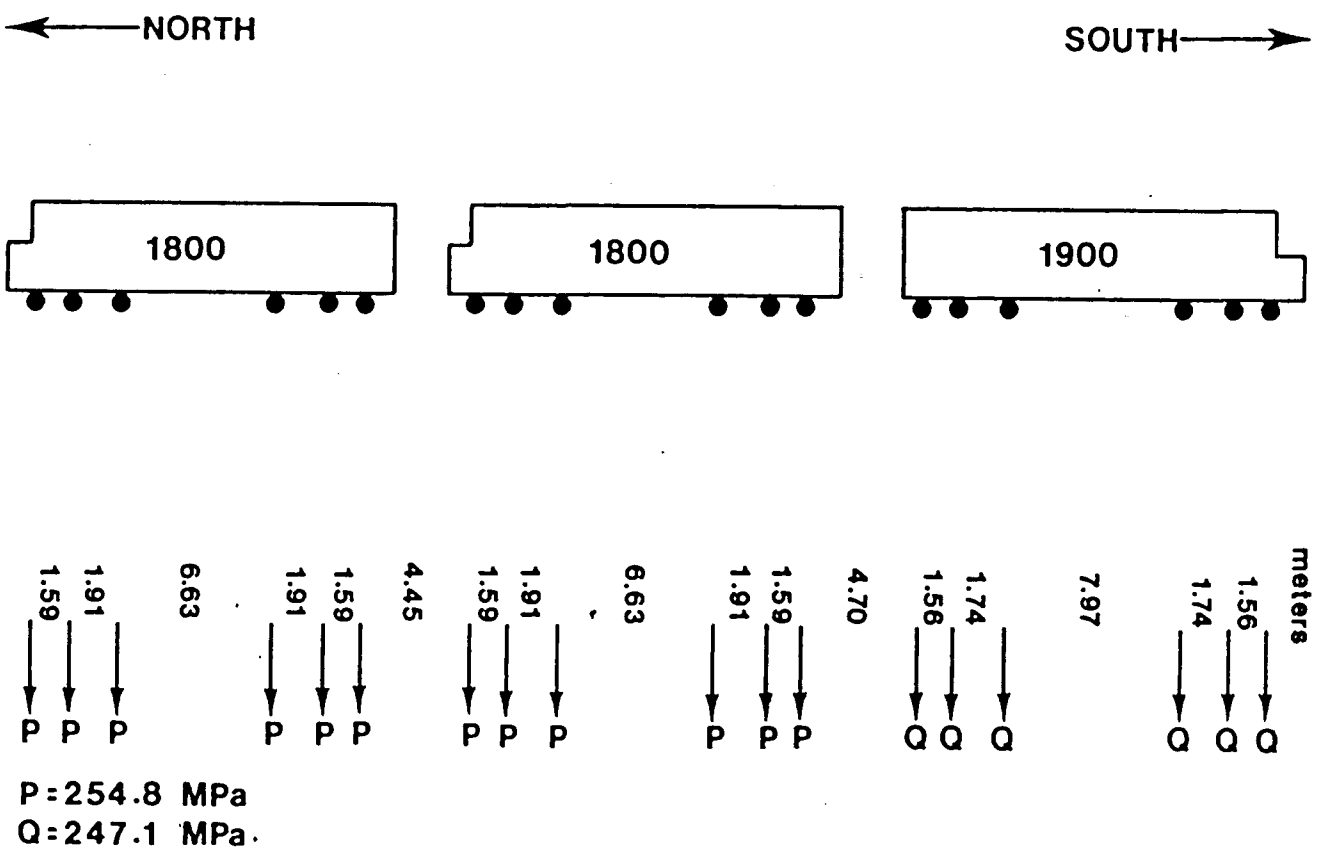

Fig. 6 Work Train Consist

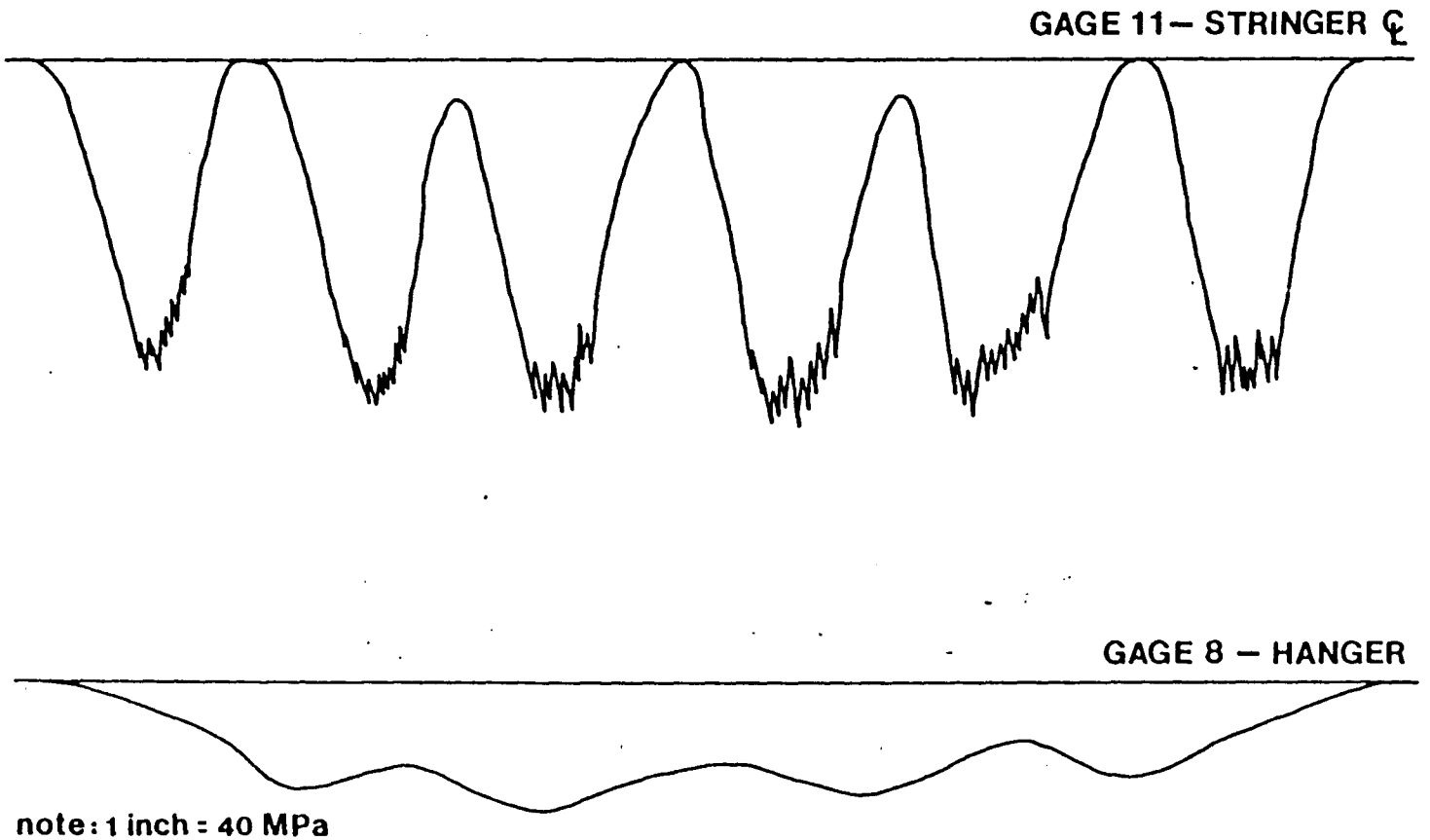

Fig. 7 Typical Analog Traces

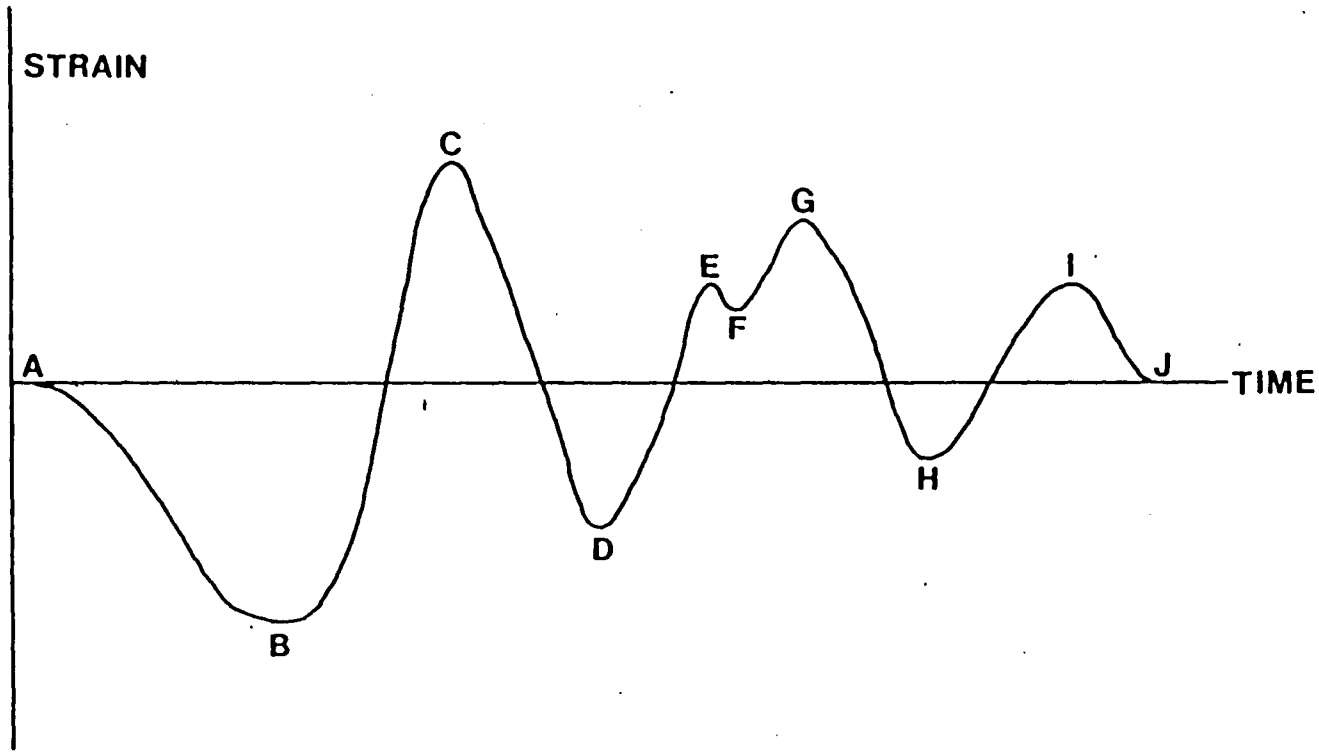

Fig. 8 Sample Strain-Time Record

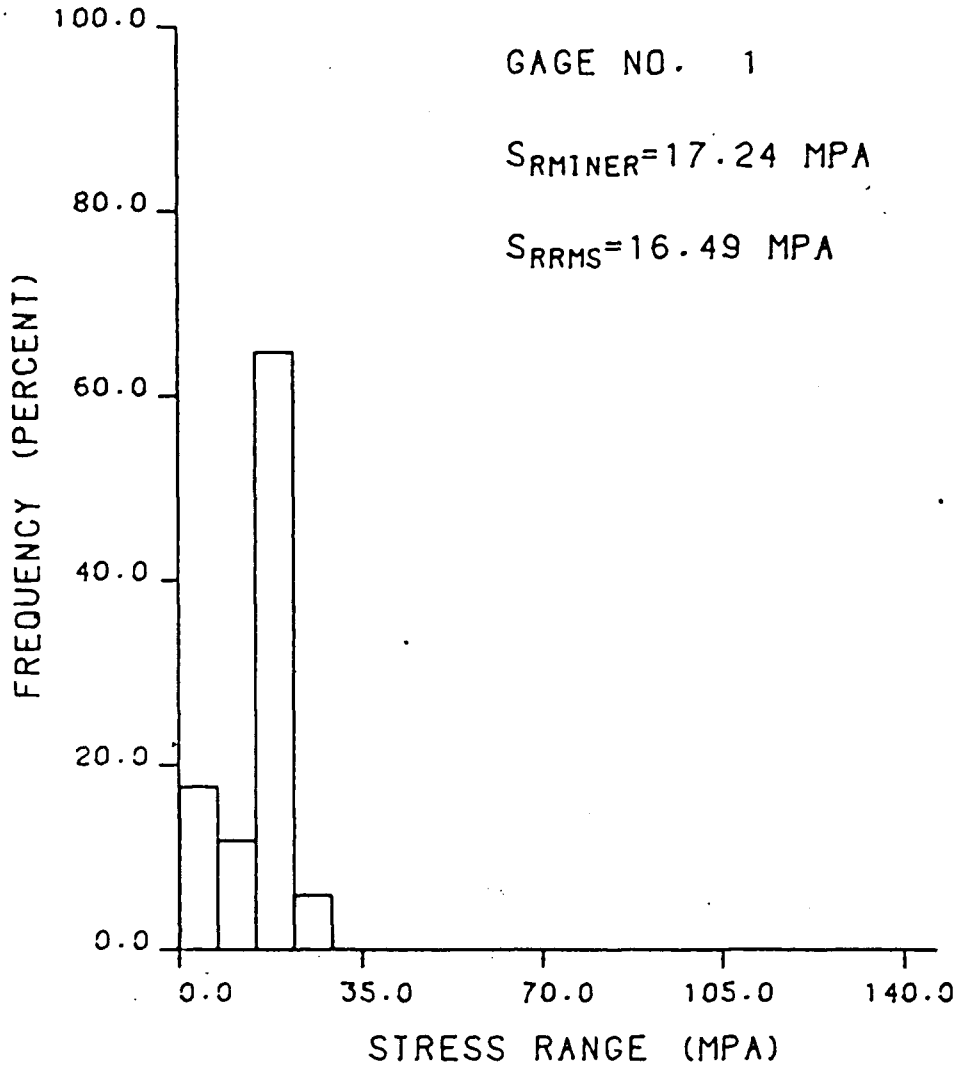

Fig. 9 Stress Range Spectrum for Gage 1

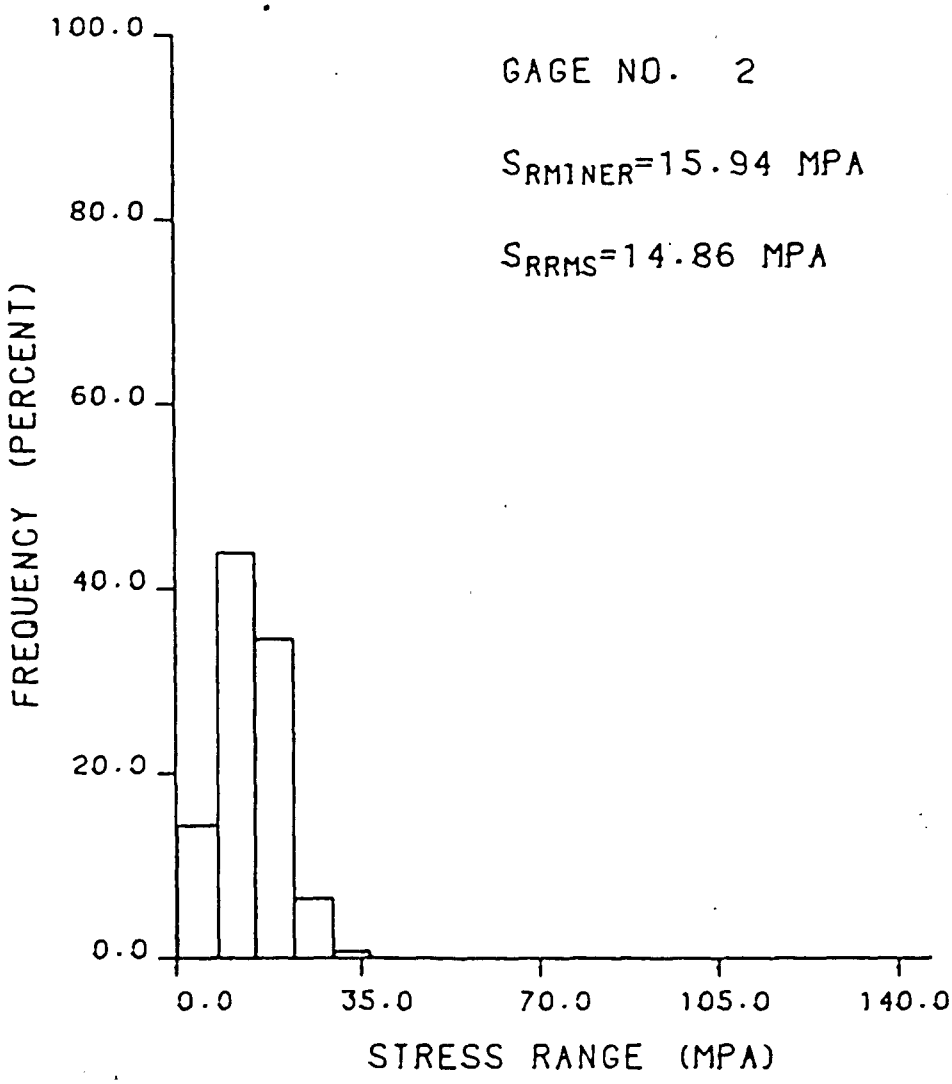

Fig. 10 Stress Range Spectrum for Gage 2

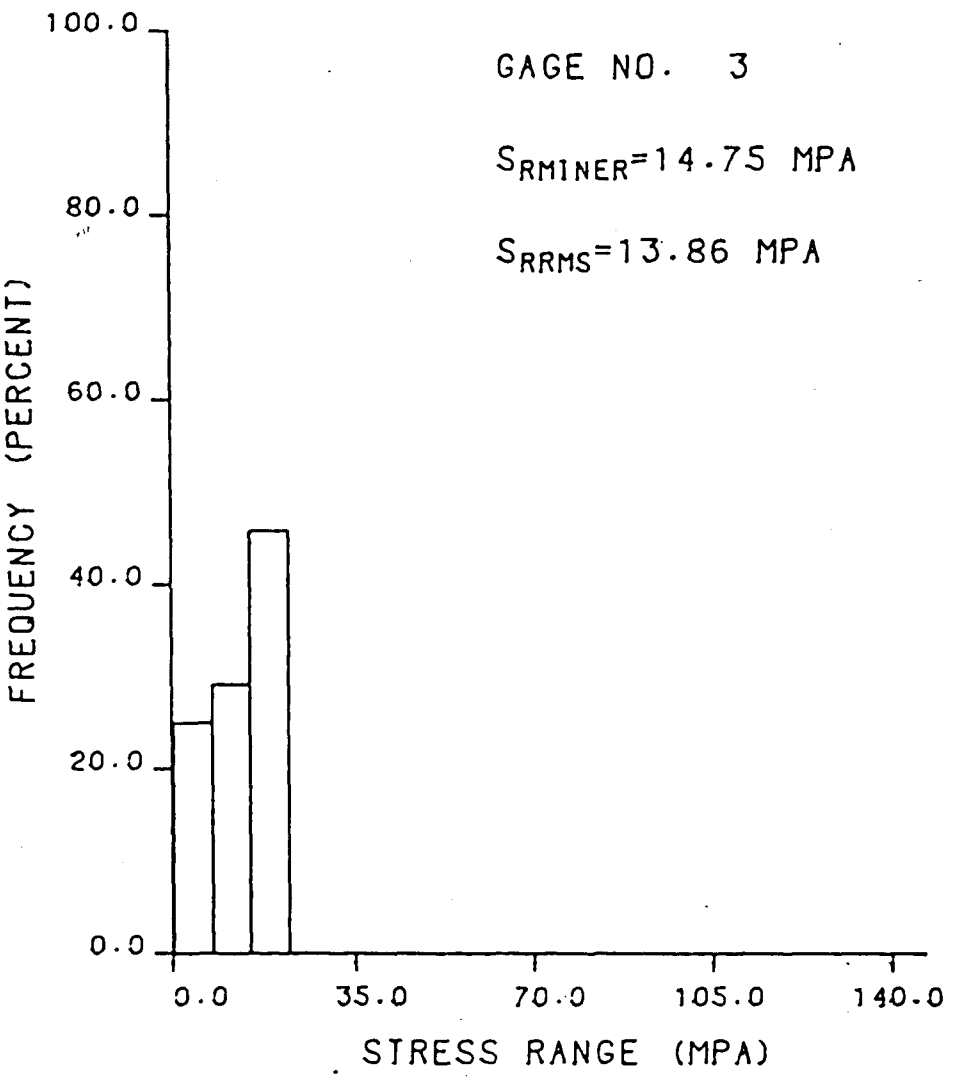

Fig. 11 Stress Range Spectrum for Gage 3

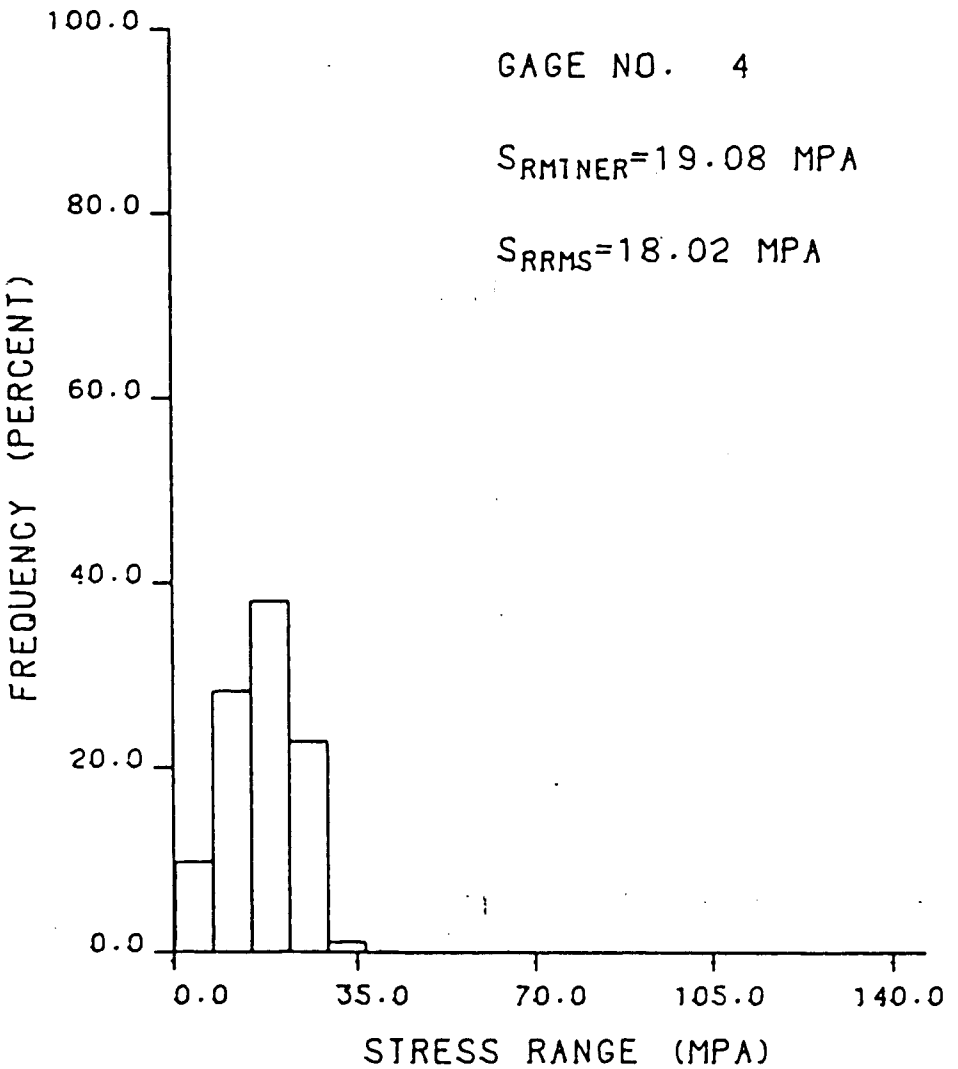

Fig. 12 Stress Range Spectrum for Gage 4

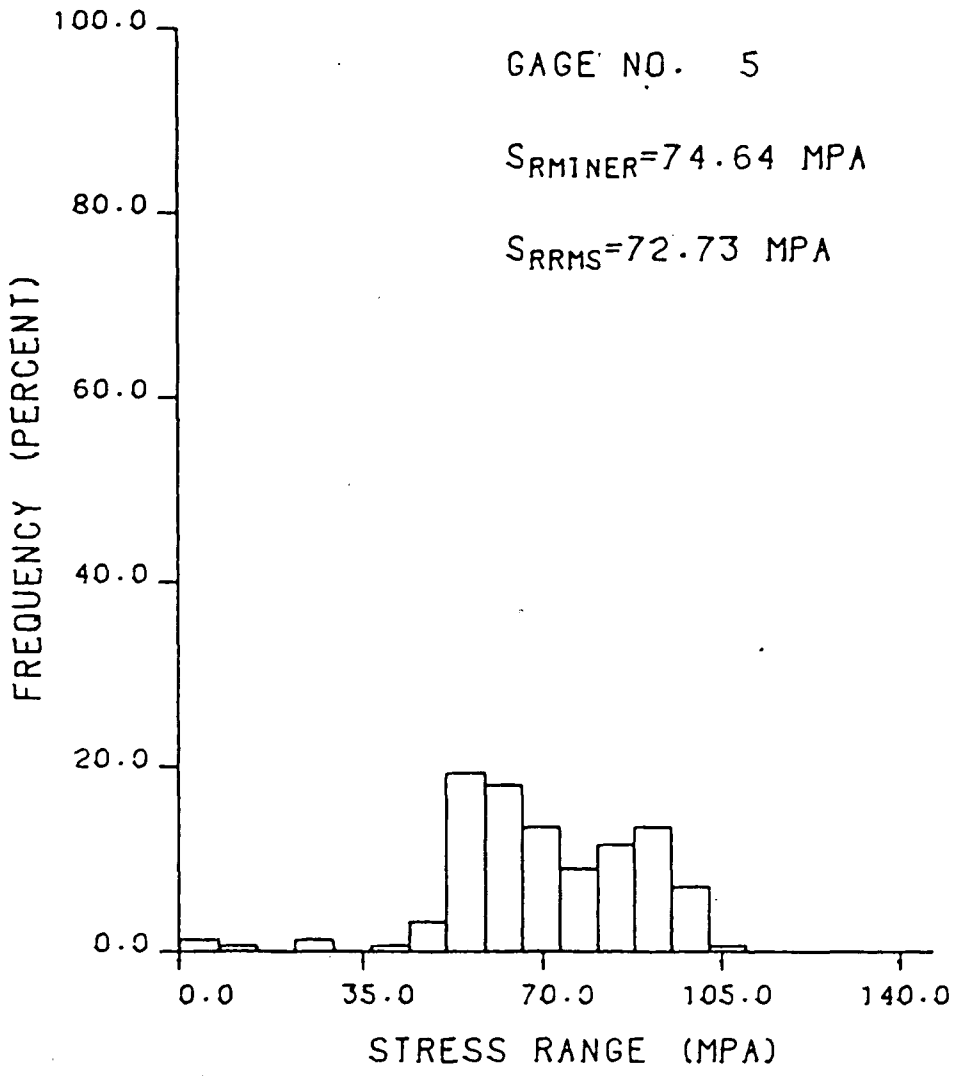

Fig. 13 Stress Range Spectrum for Gage 5

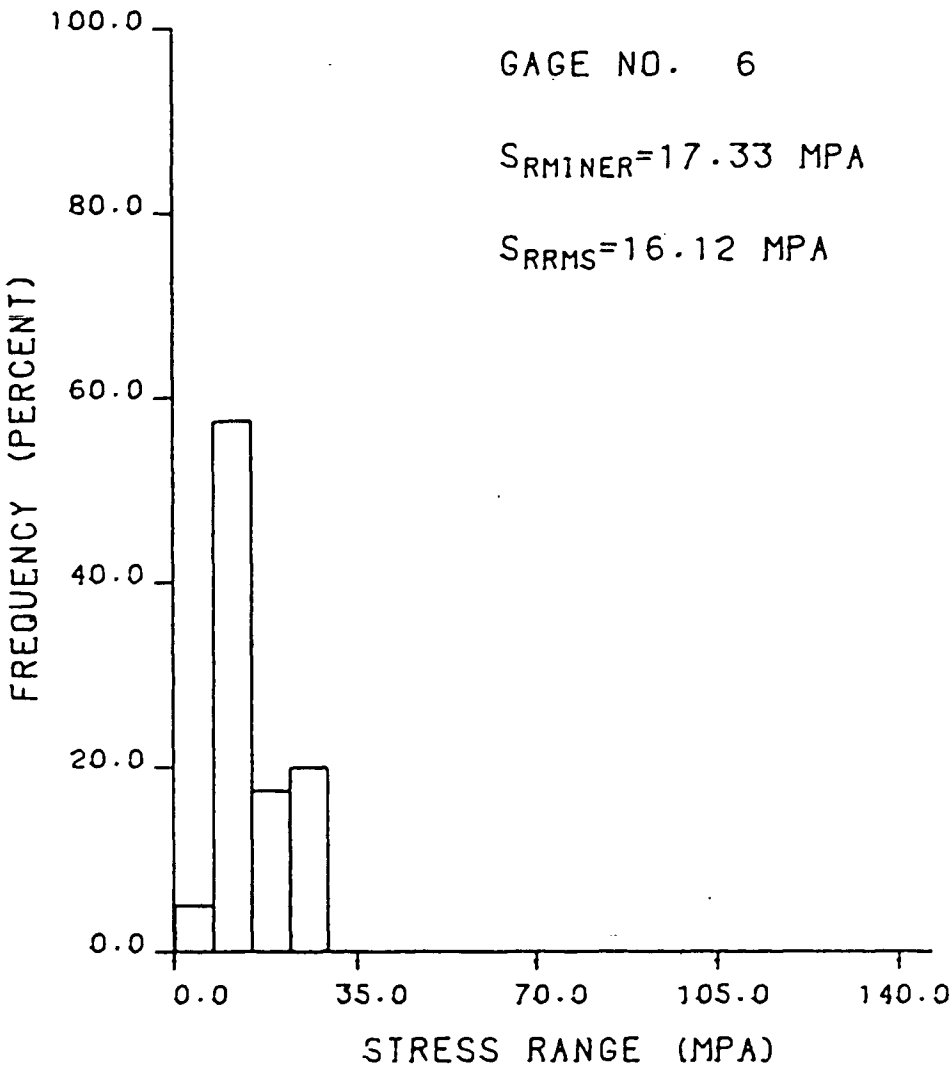

Fig. 14 Stress Range Spectrum for Gage 6

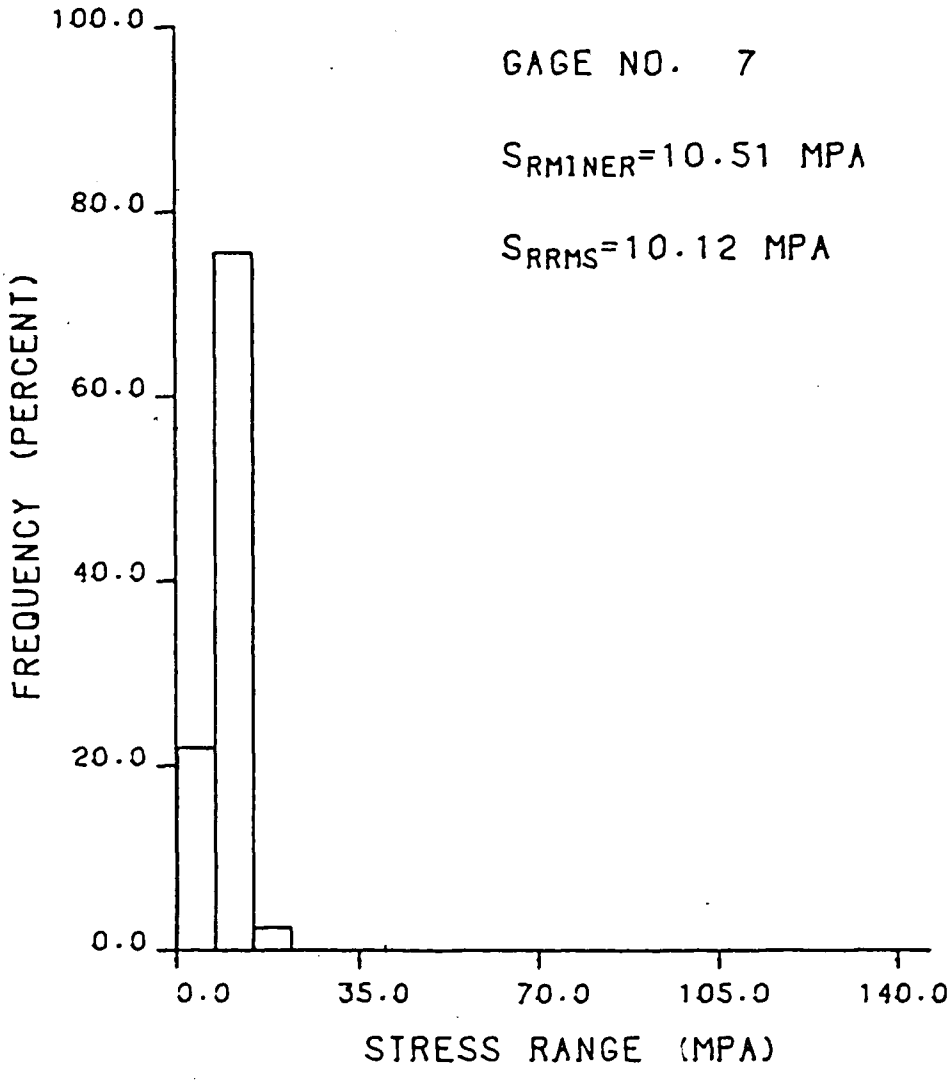

Fig. 15 Stress Range Spectrum for Gage 7

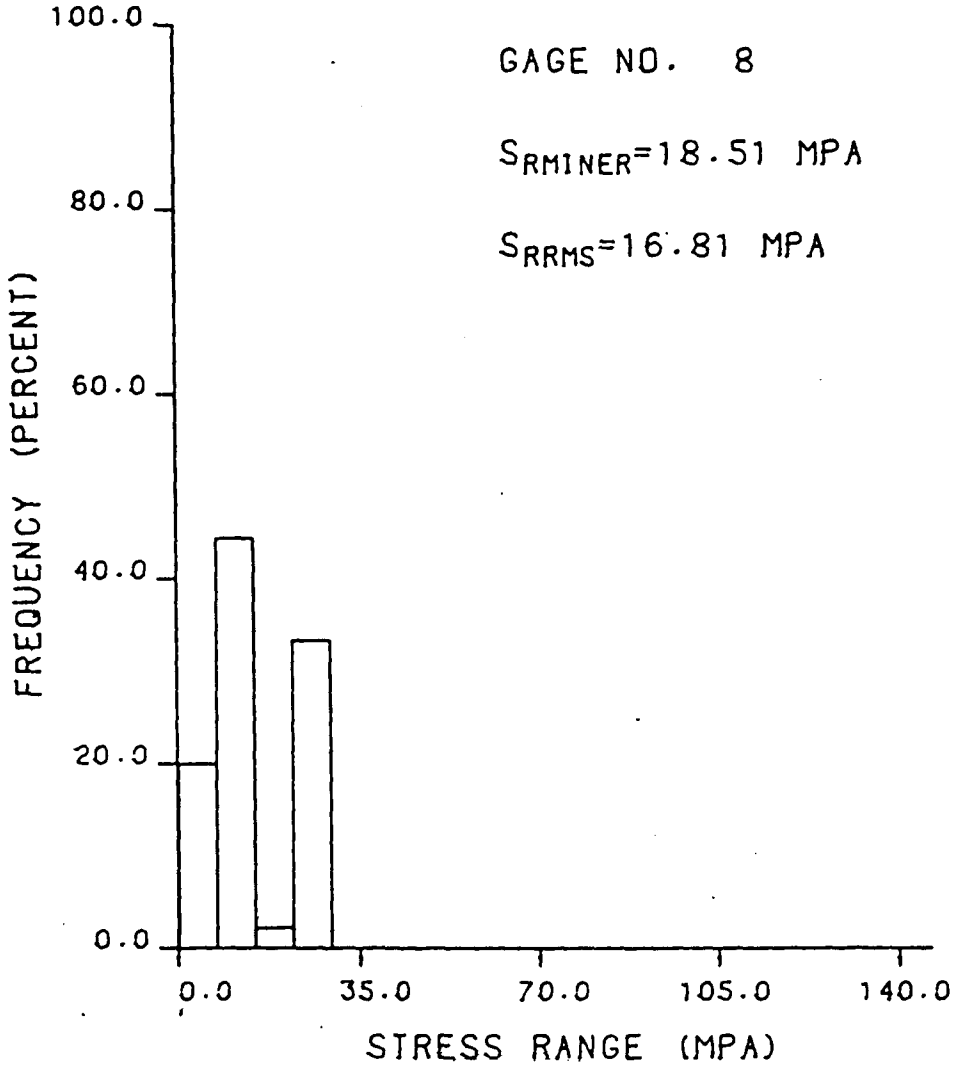

Fig. 16 Stress Range Spectrum for Gage 8

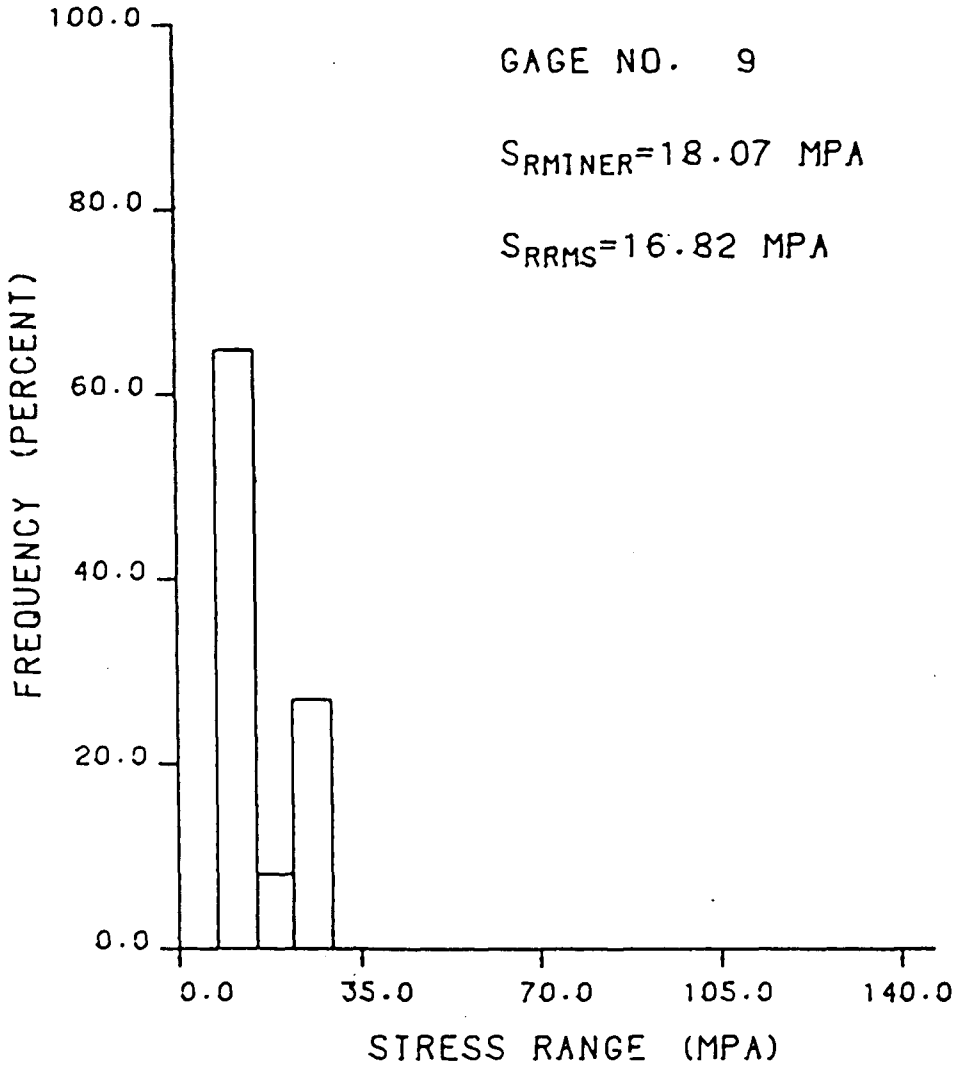

Fig. 17 Stress Range Spectrum for Gage 9

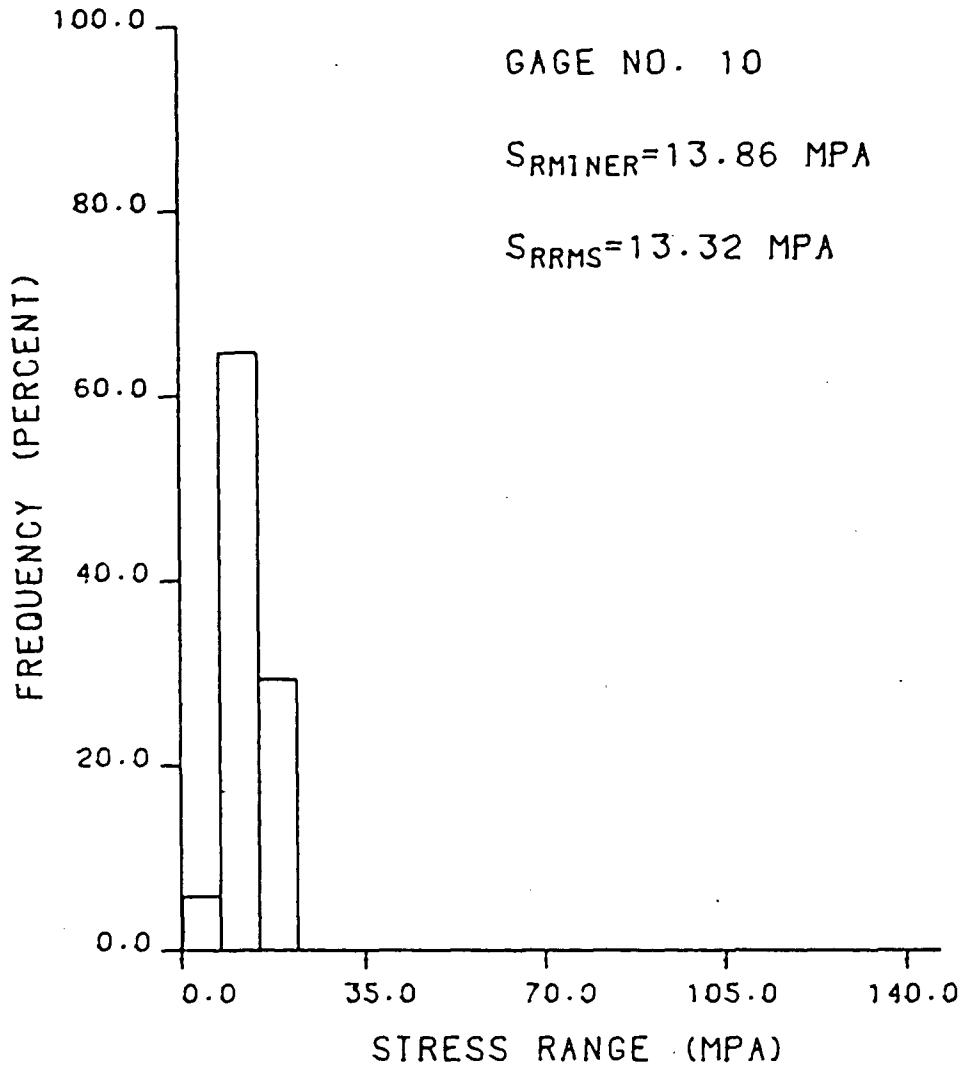

Fig. 18 Stress Range Spectrum for Gage 10

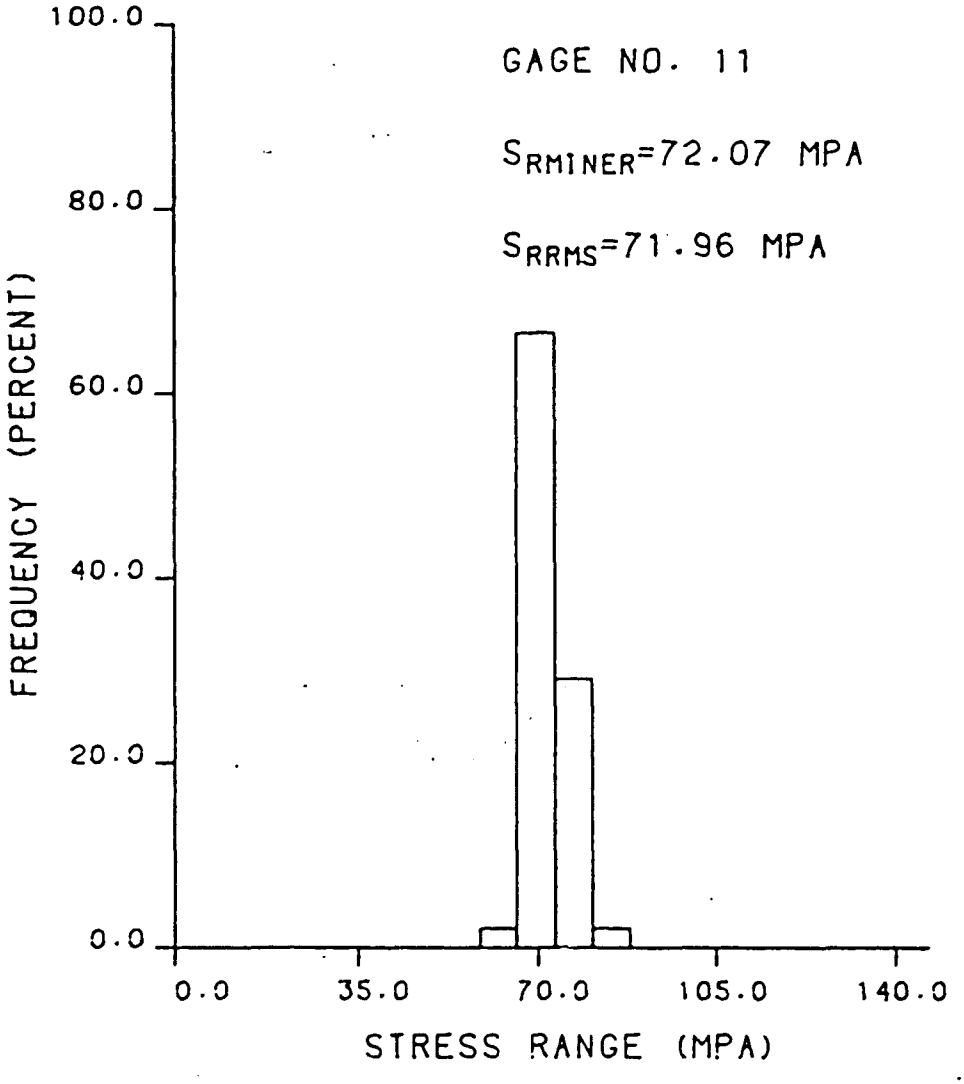

Fig. 19 Stress Range Spectrum for Gage 11

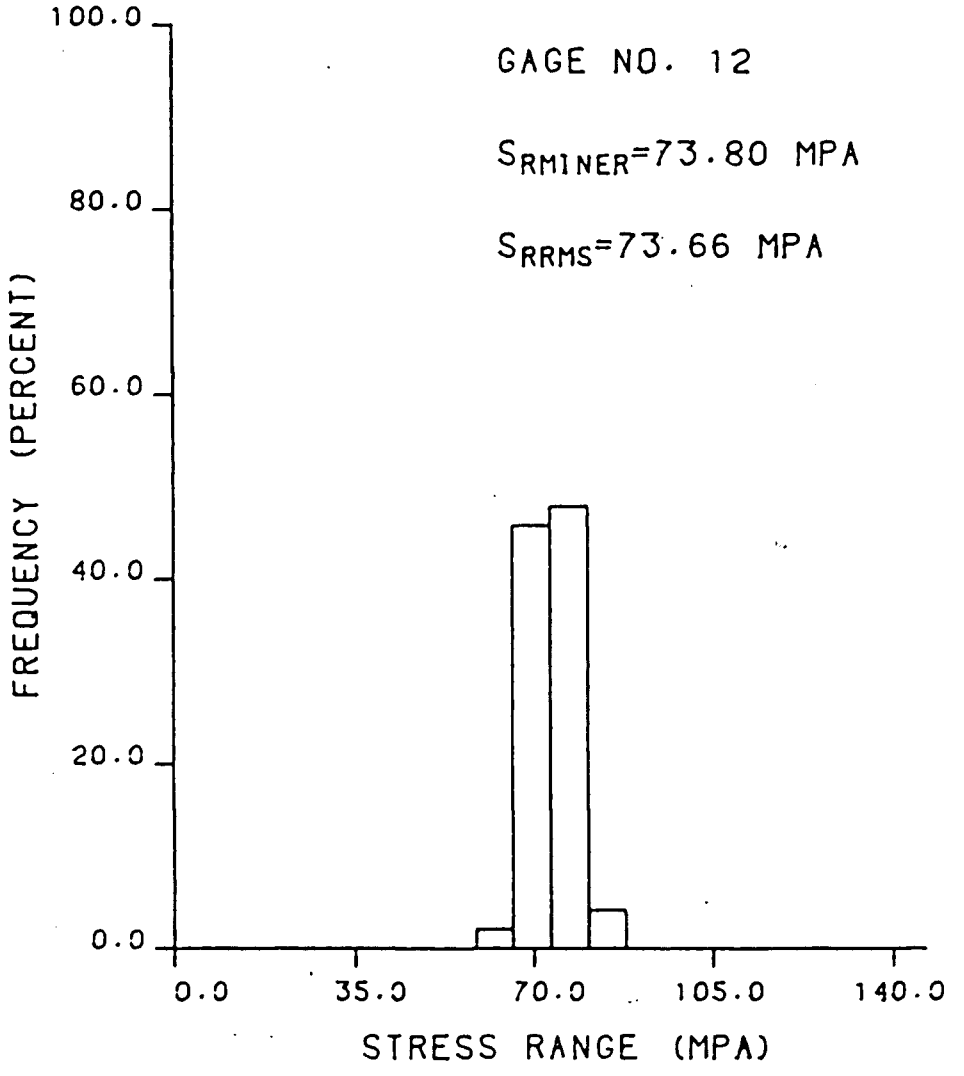

Fig. 20 Stress Range Spectrum for Gage 12

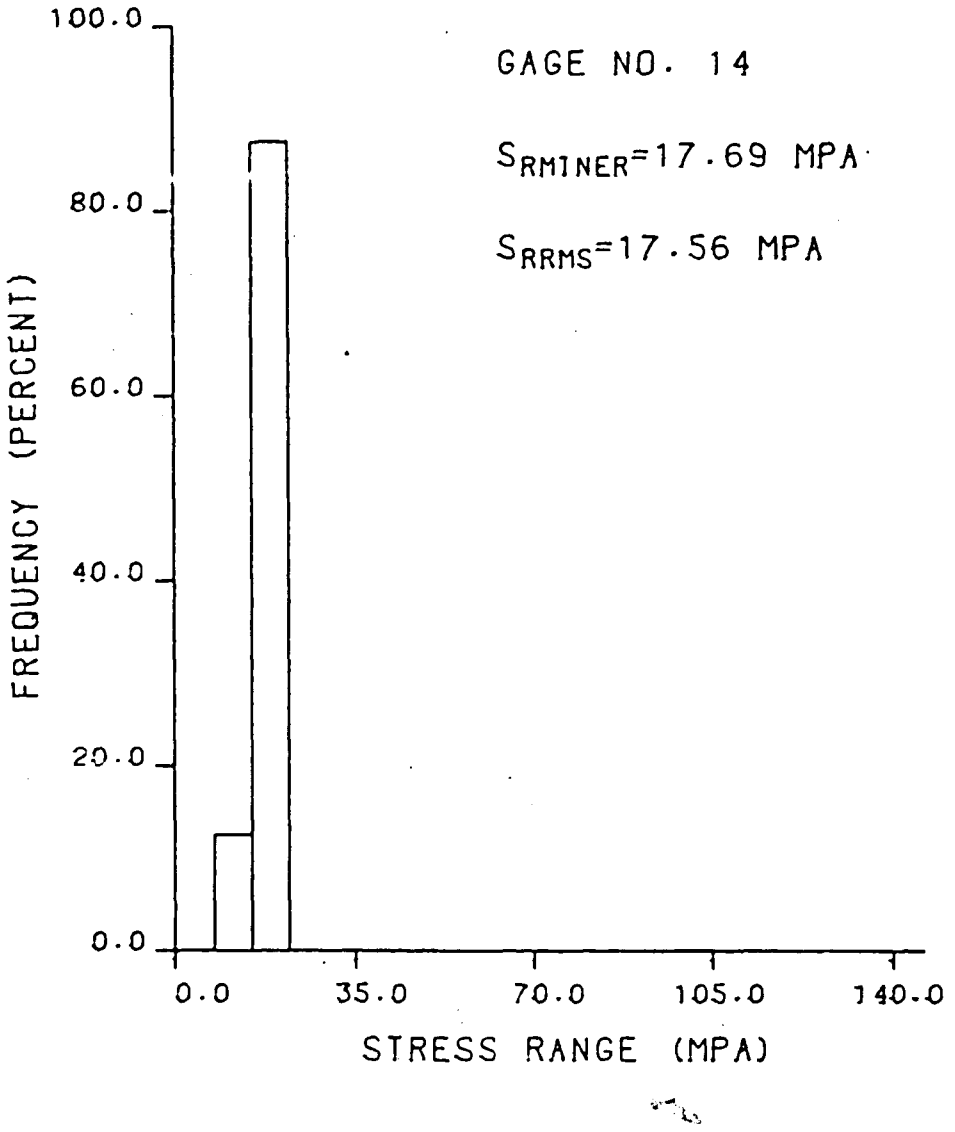

Fig. 21 Stress Range Spectrum for Gage 14

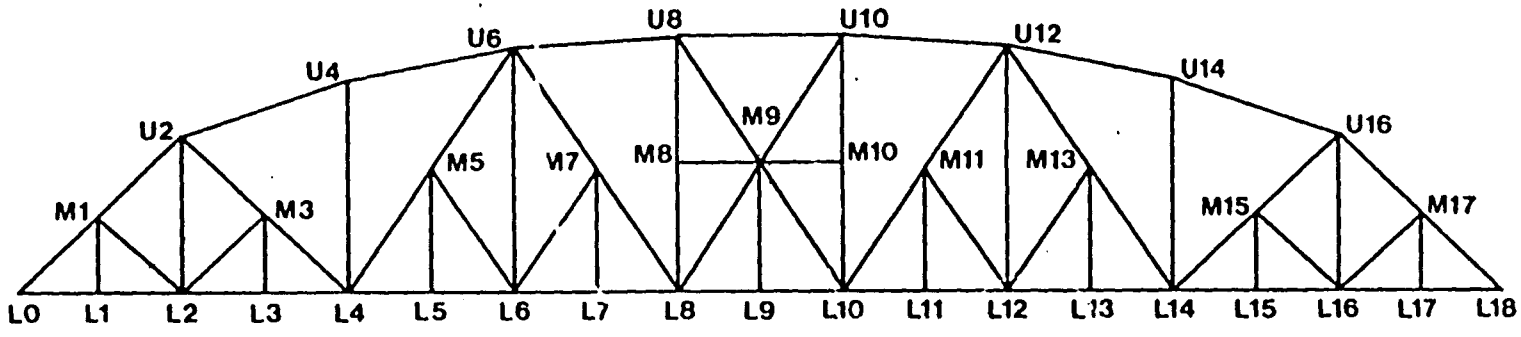

Fig. 22 Plane Truss and Plane Frame Model

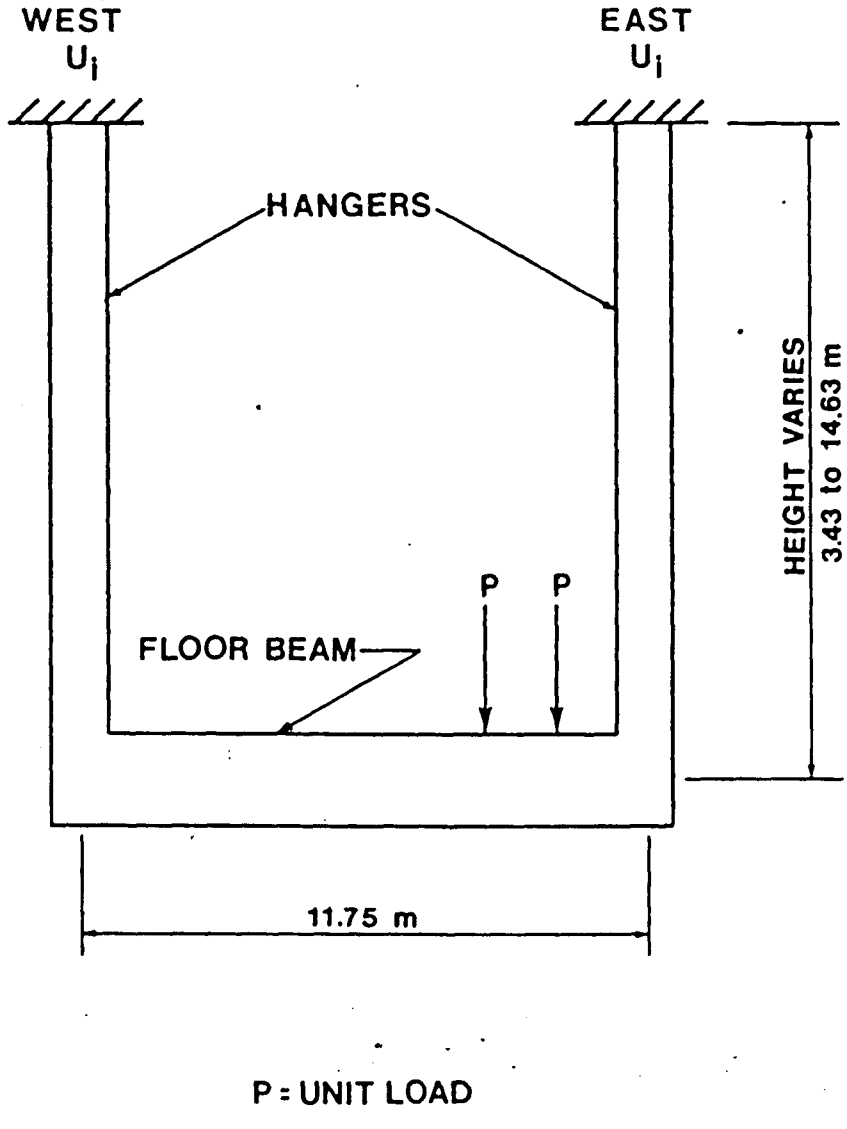

Fig. 23 Floor Beam and Hanger Frame Model

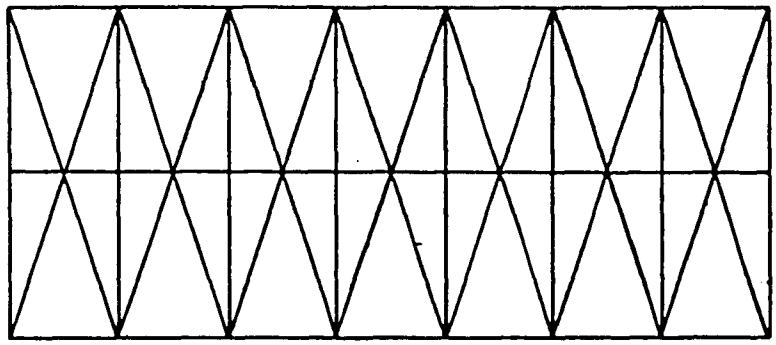

TOP LATERAL SYSTEM

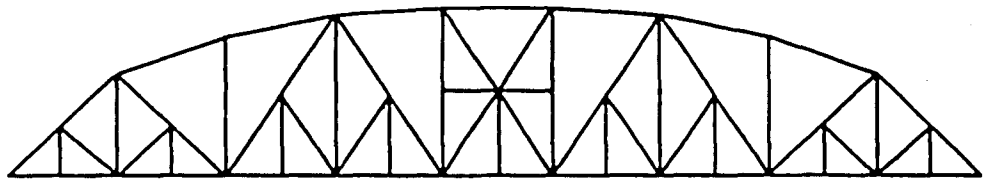

EAST AND WEST TRUSSES

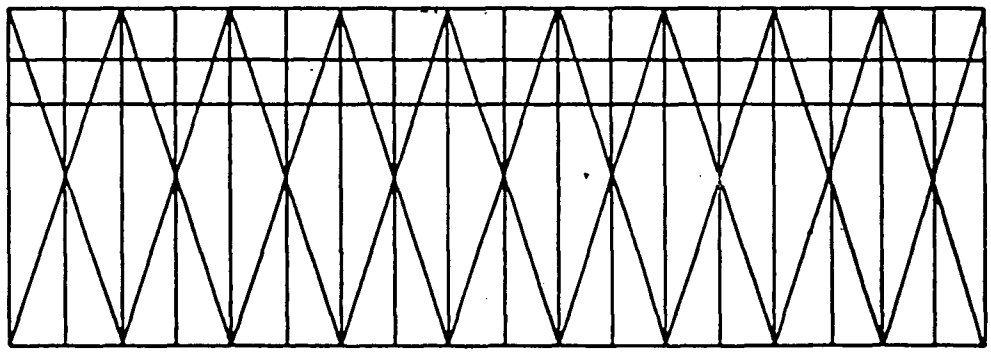

FLOOR SYSTEM

Fig. 24 Schematic of Space Frame Model

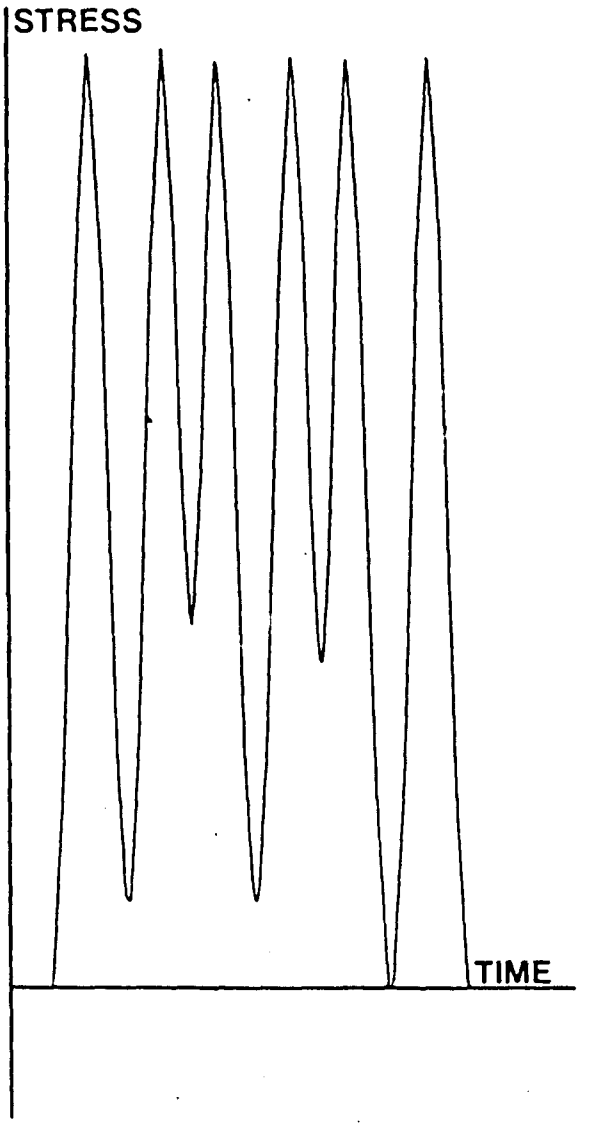

Fig. 25 Stress-Time Curve for Stringer (Gage 11) in Space Frame Model Due to Work Train Consist

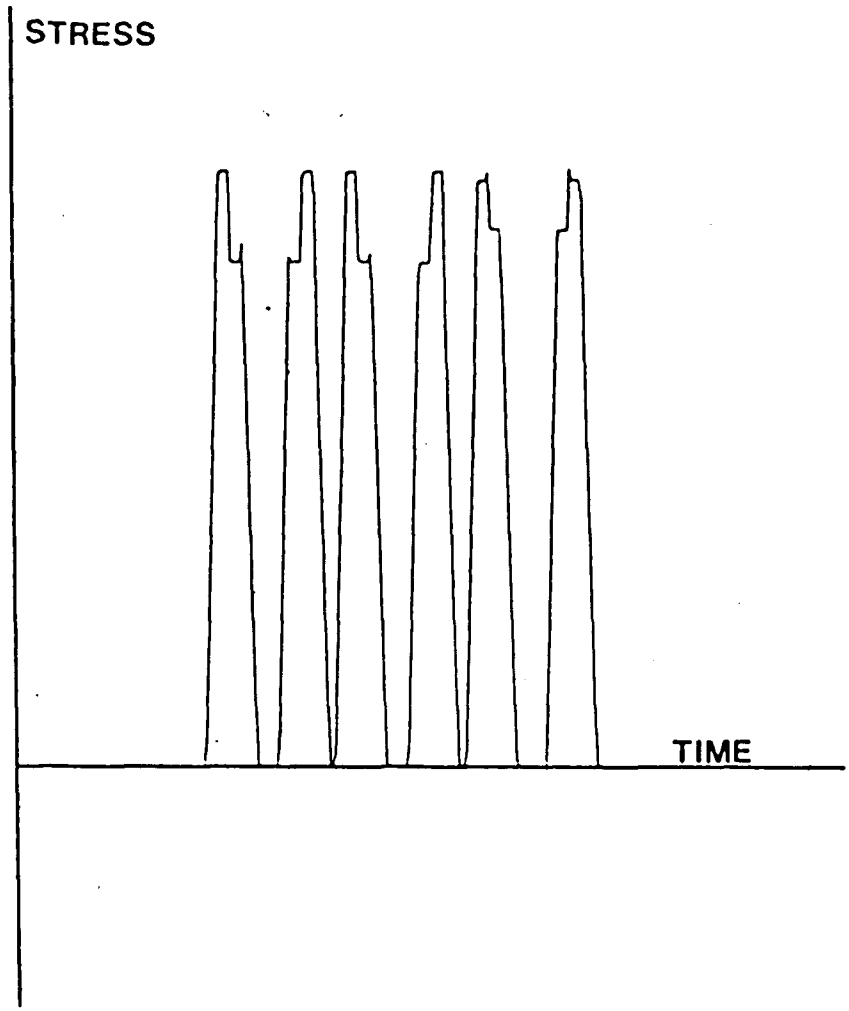

Fig. 26 Stress-Time Curve for Stringer (Gage 11) in Simple Beam Model Due to Work Train Consist

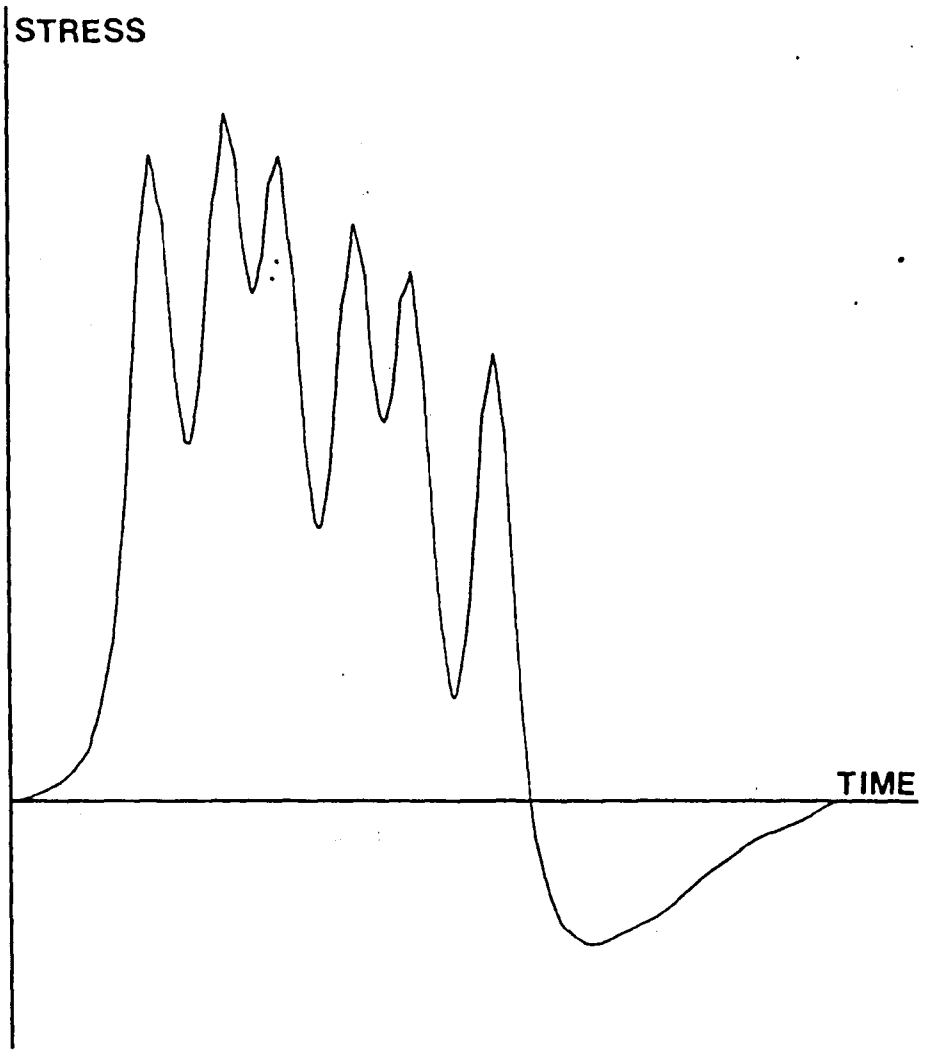

Fig. 27 Stress-Time Curve for Floor Beam (Gage 10) in Space Frame Model Due to Work Train Consist

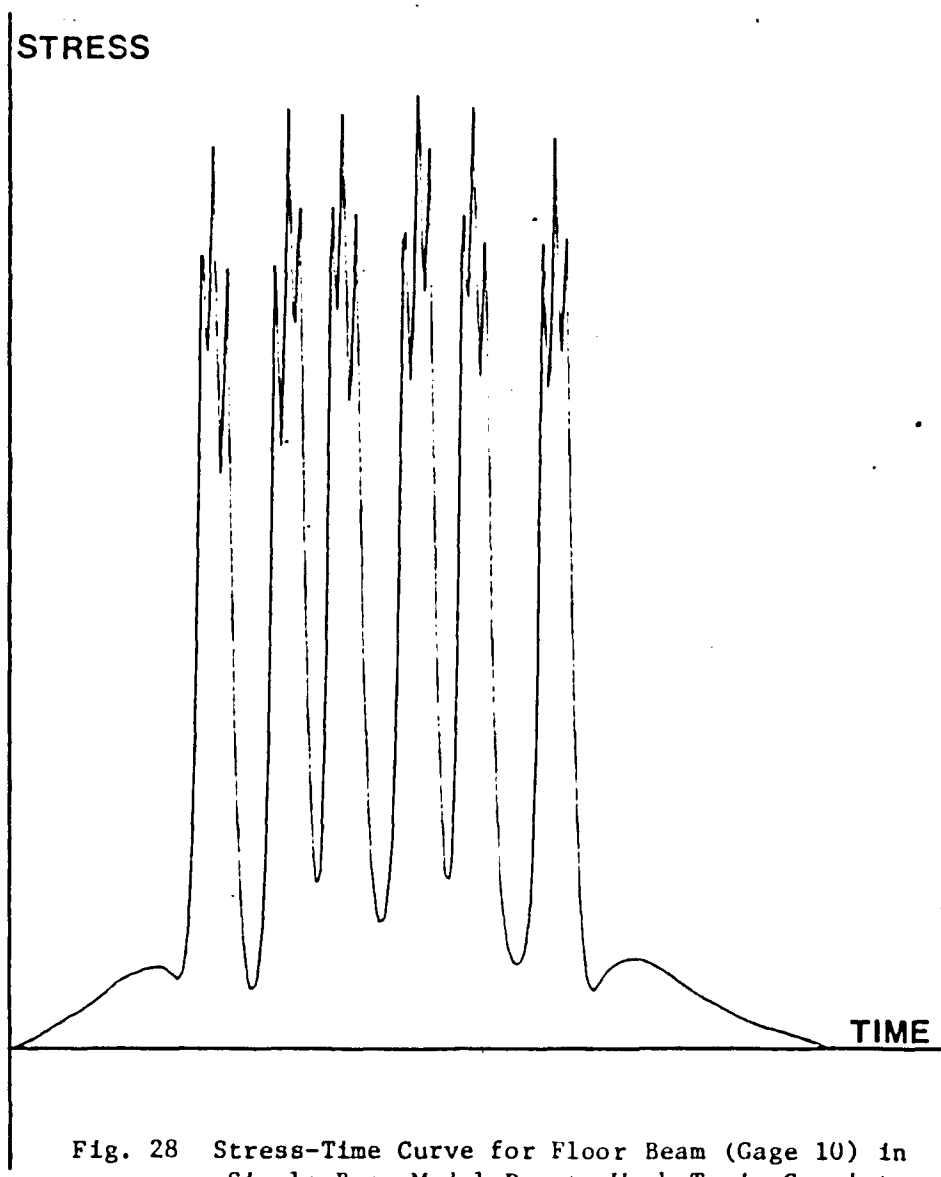

Fig. 28 Stress-Time Curve for Floor Beam (Gage 10) in Simple Beam Model Due to Work Train Consist

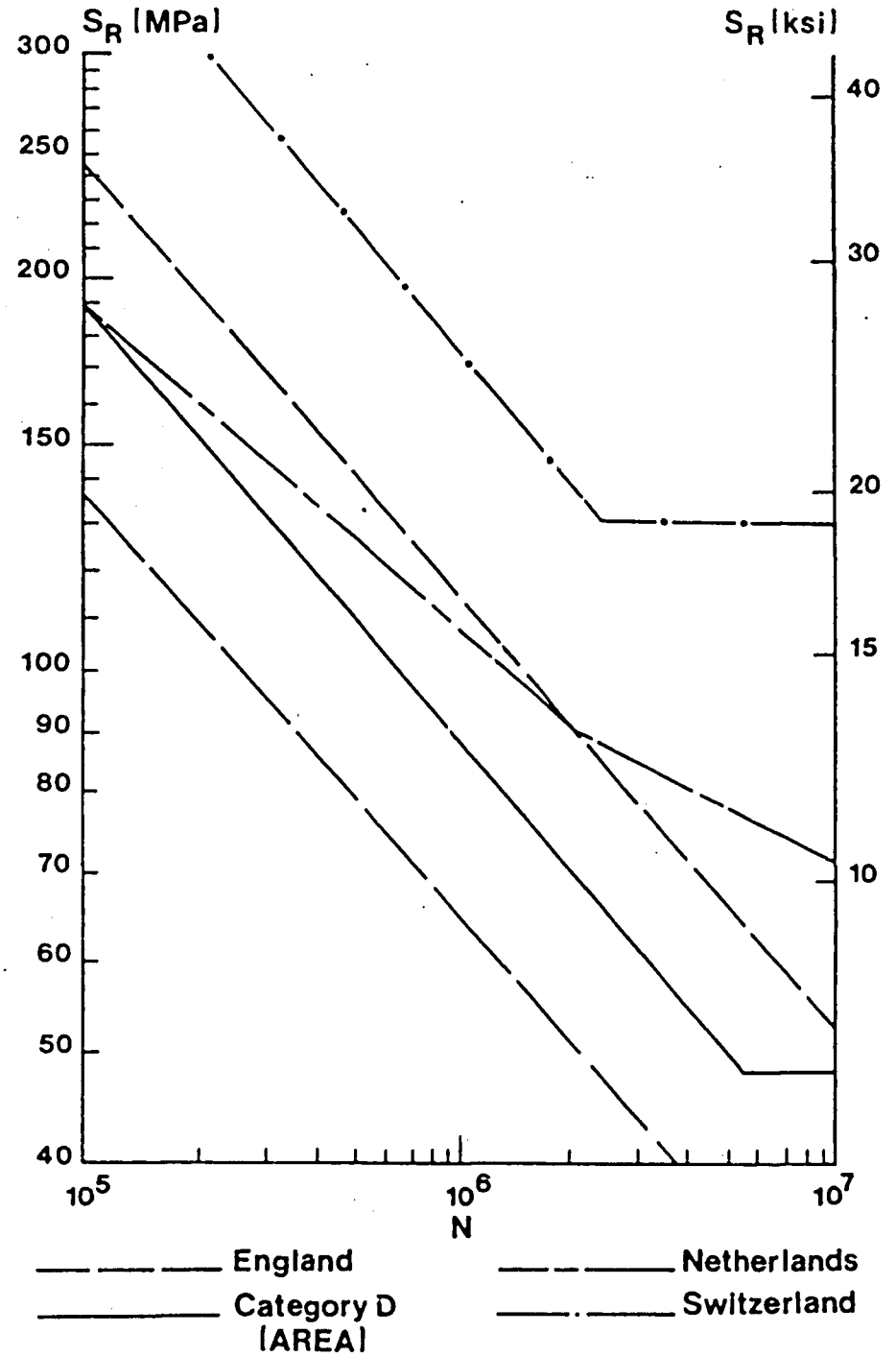

Fig. 29 Fatigue Resistance Curves for Riveted Connections

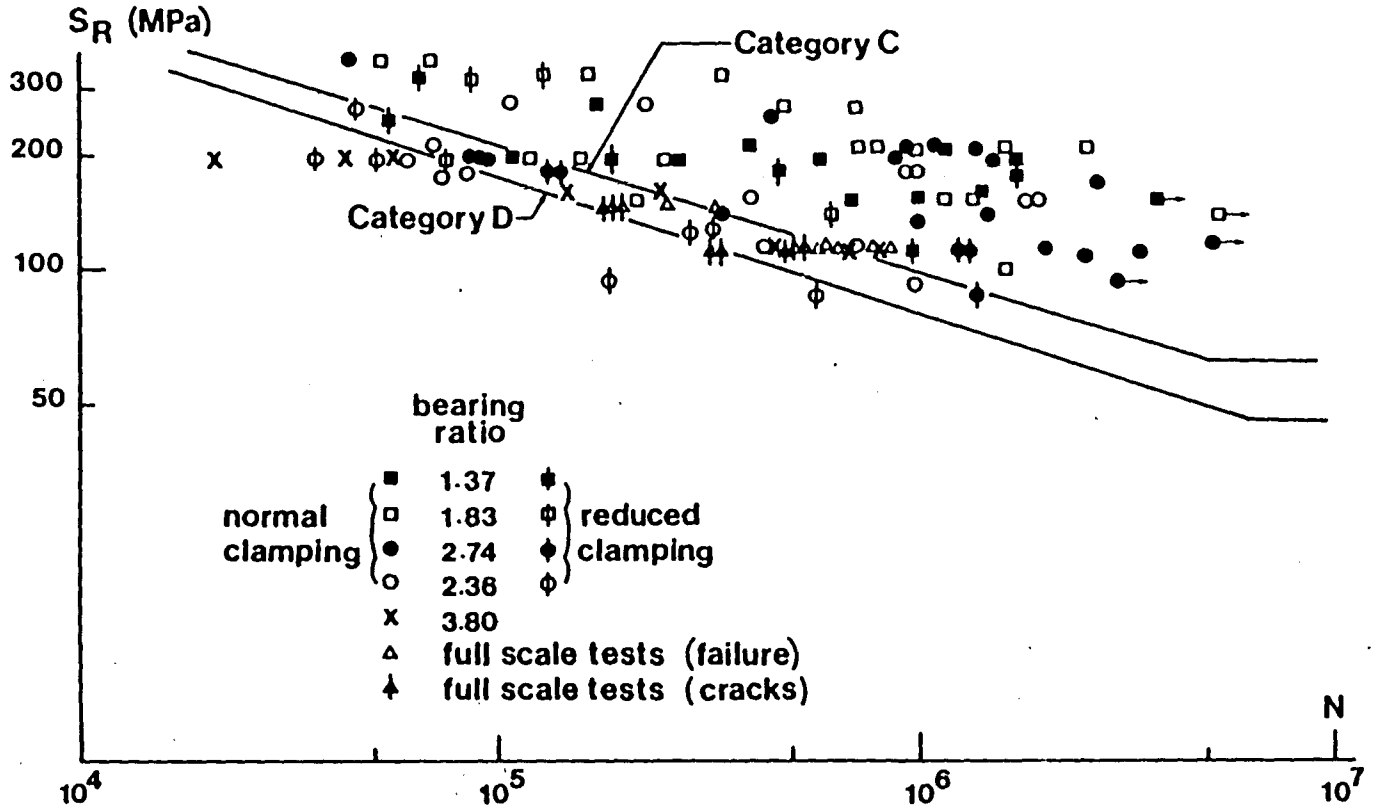

Fig. 30 Fatigue Strength of Riveted Connections (AREA, 1980)

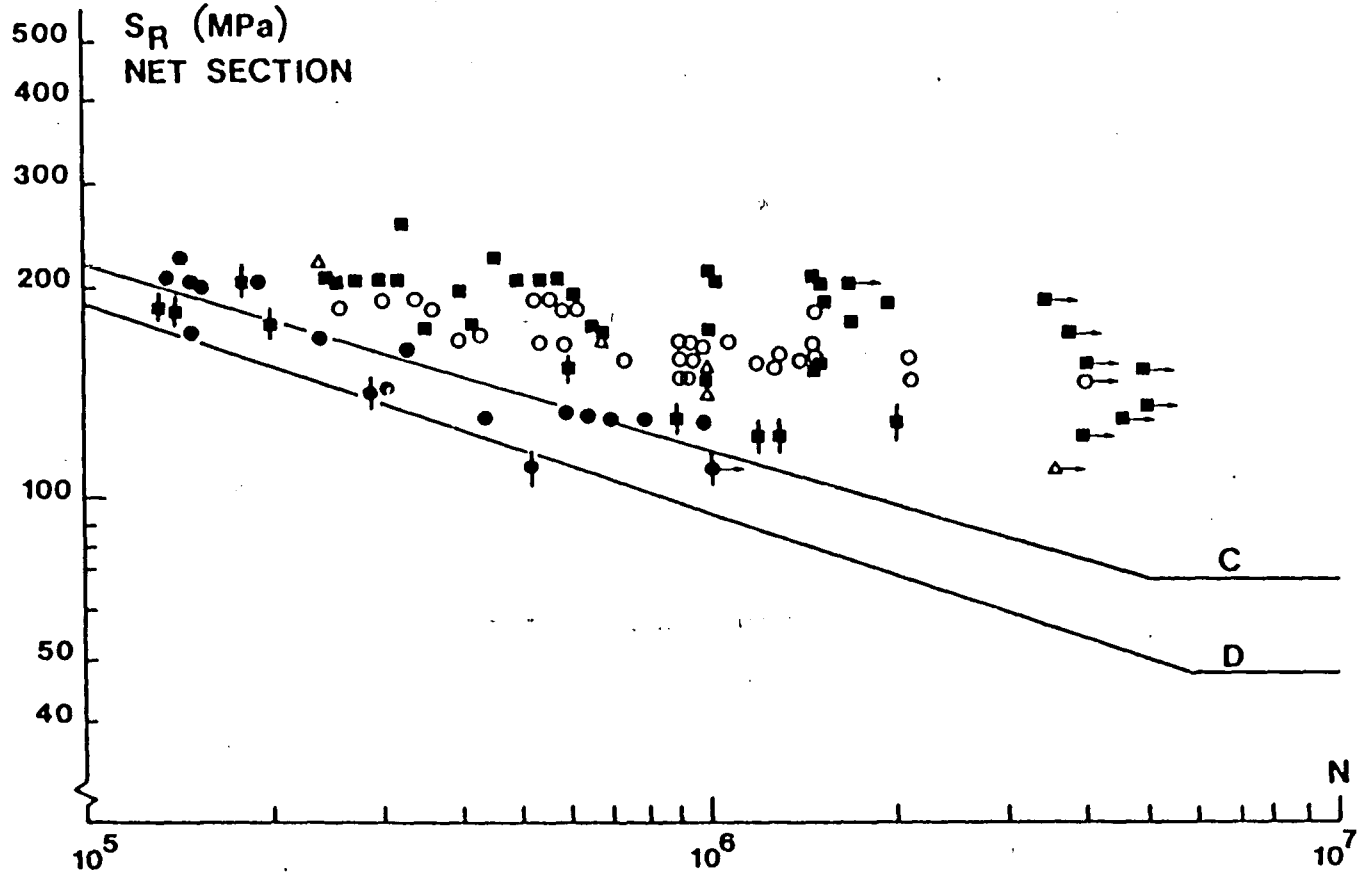

Fig. 31 Fatigue Strength of Riveted Connections Subjected to Zero-to-Tension Loading

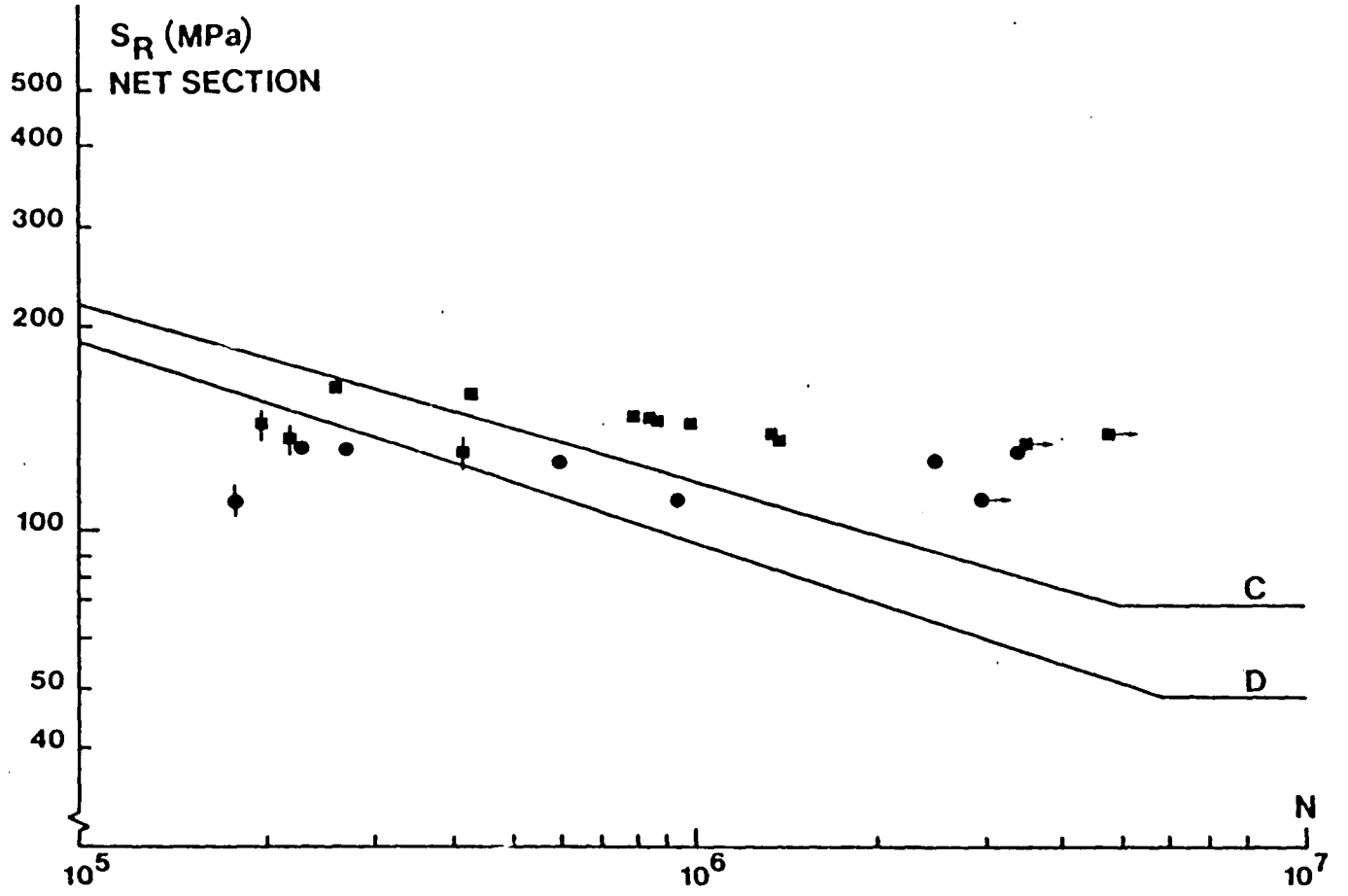

Fig. 32 Fatigue Strength of Riveted Connections Subjected to Half Tension-to-Tension Loading

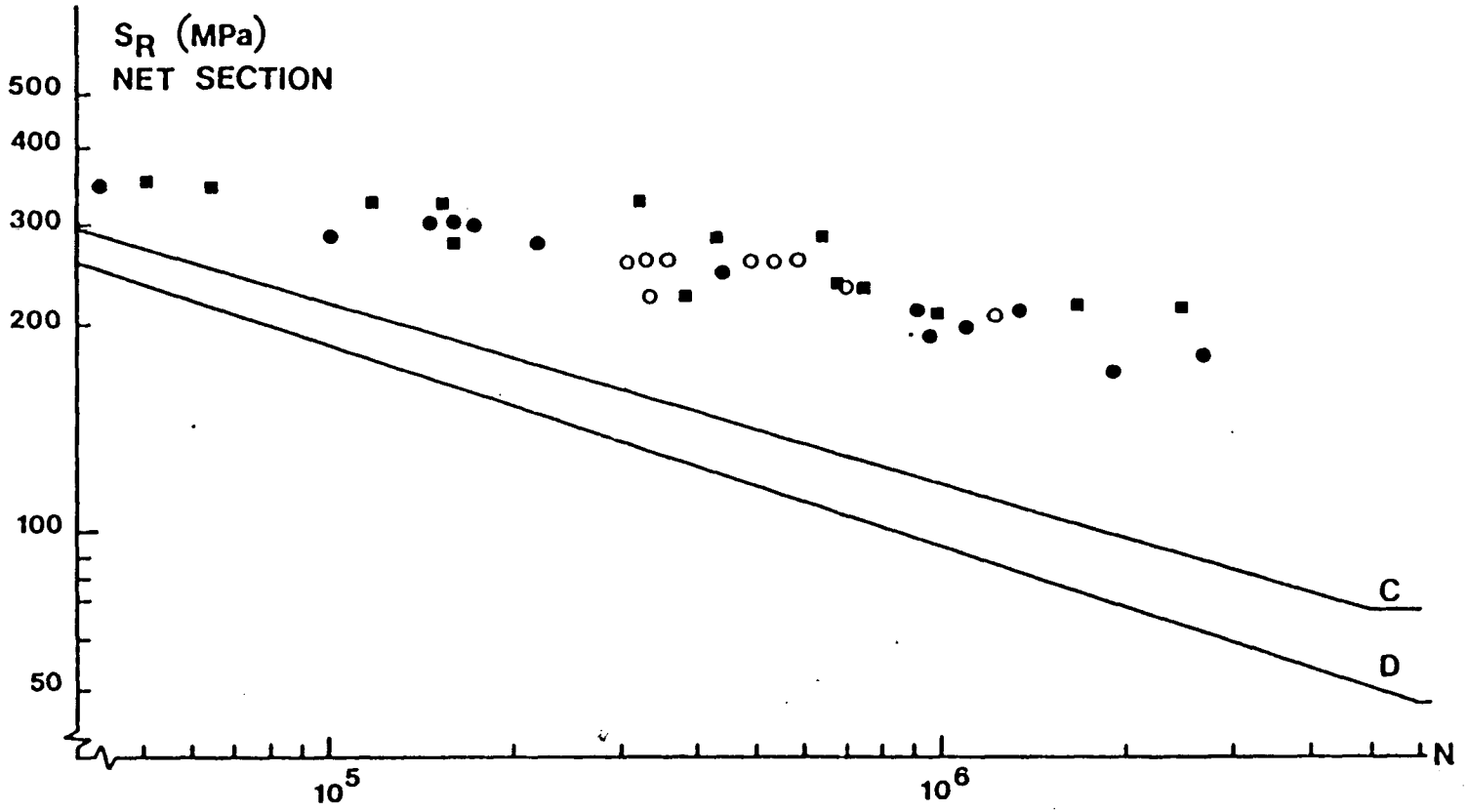

Fig. 33 Fatigue Strength of Riveted Connectionge Subjected to Full Reversal Loading ($S_R = S_{MAX} - S_{MIN}$)

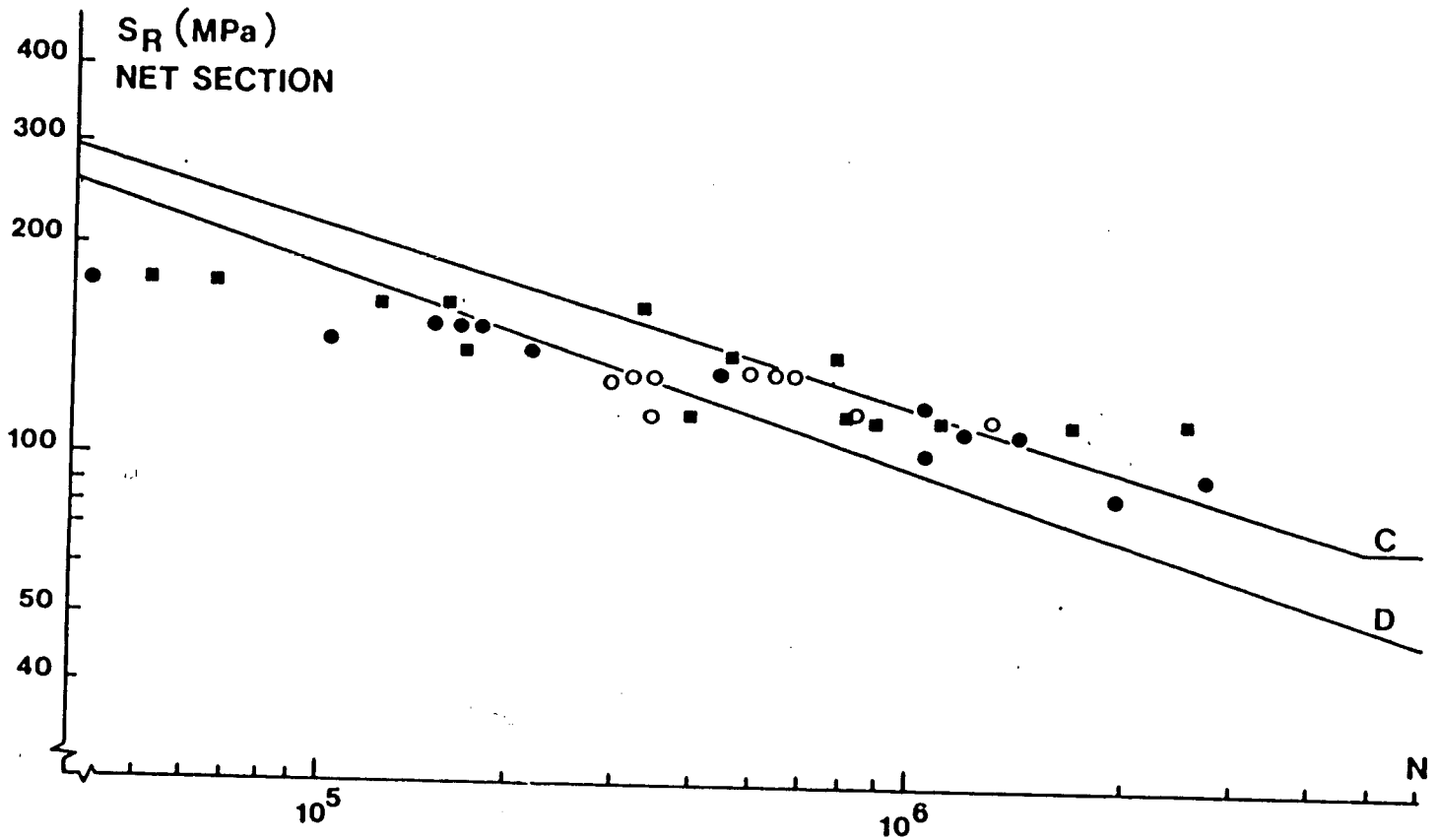

Fig. 34 Fatigue Strength of Rivered Connections Subjected to Full Reversal Loading ($S_R = S_{MAX}$)

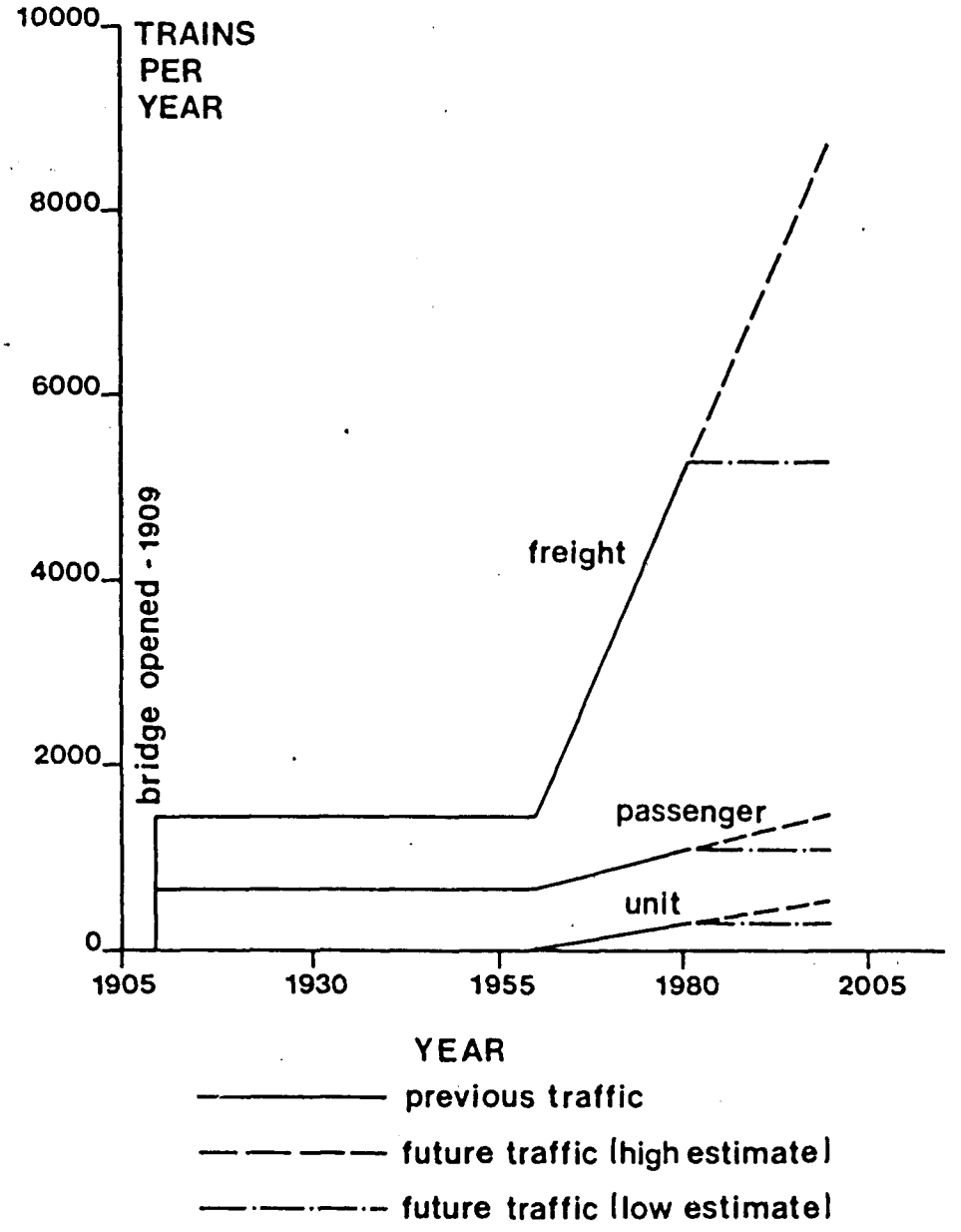

Fig. 35 Estimated Past and Future Train Traffic on the Blue Nile Bridge

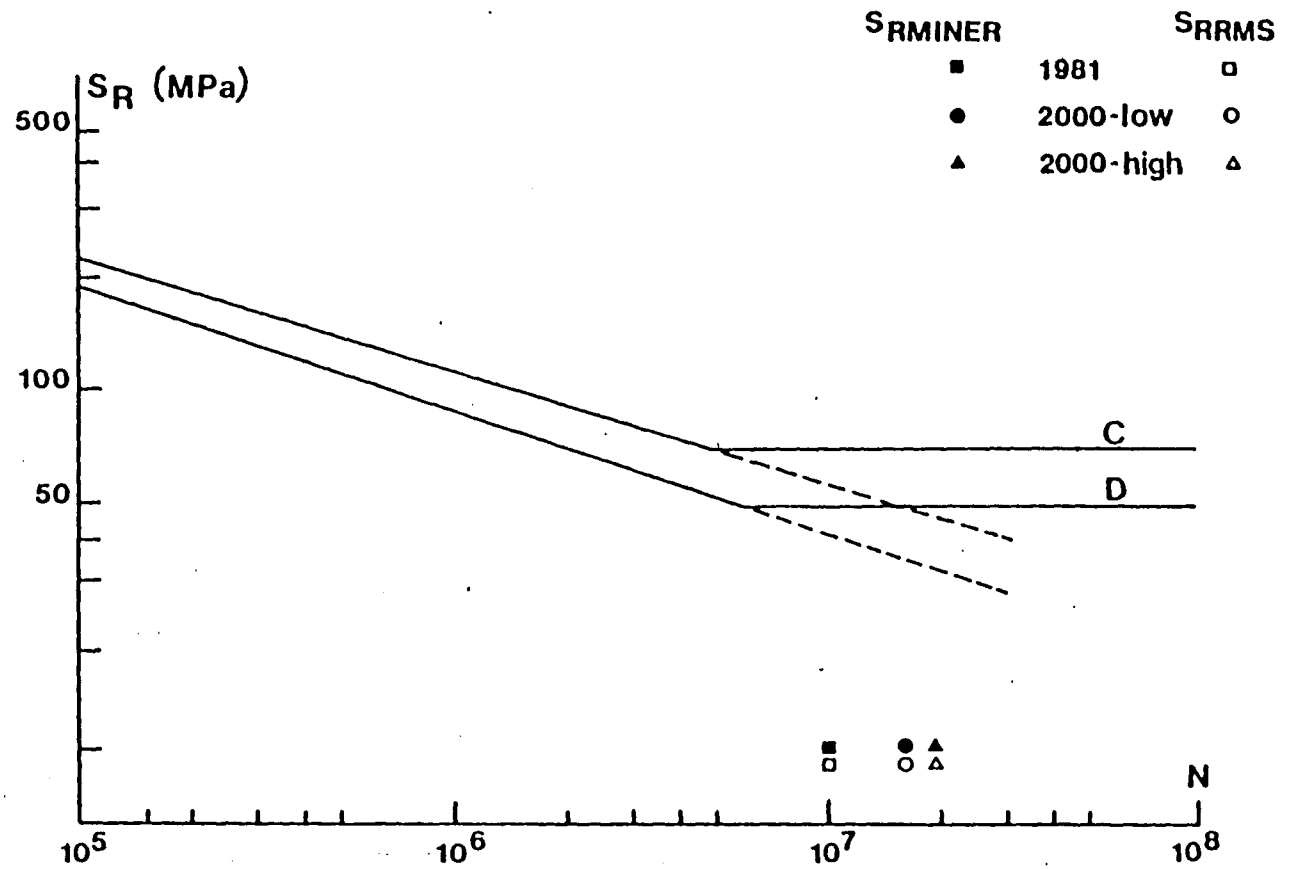

Fig. 36 Fatigue Life of Critical Floor Beam

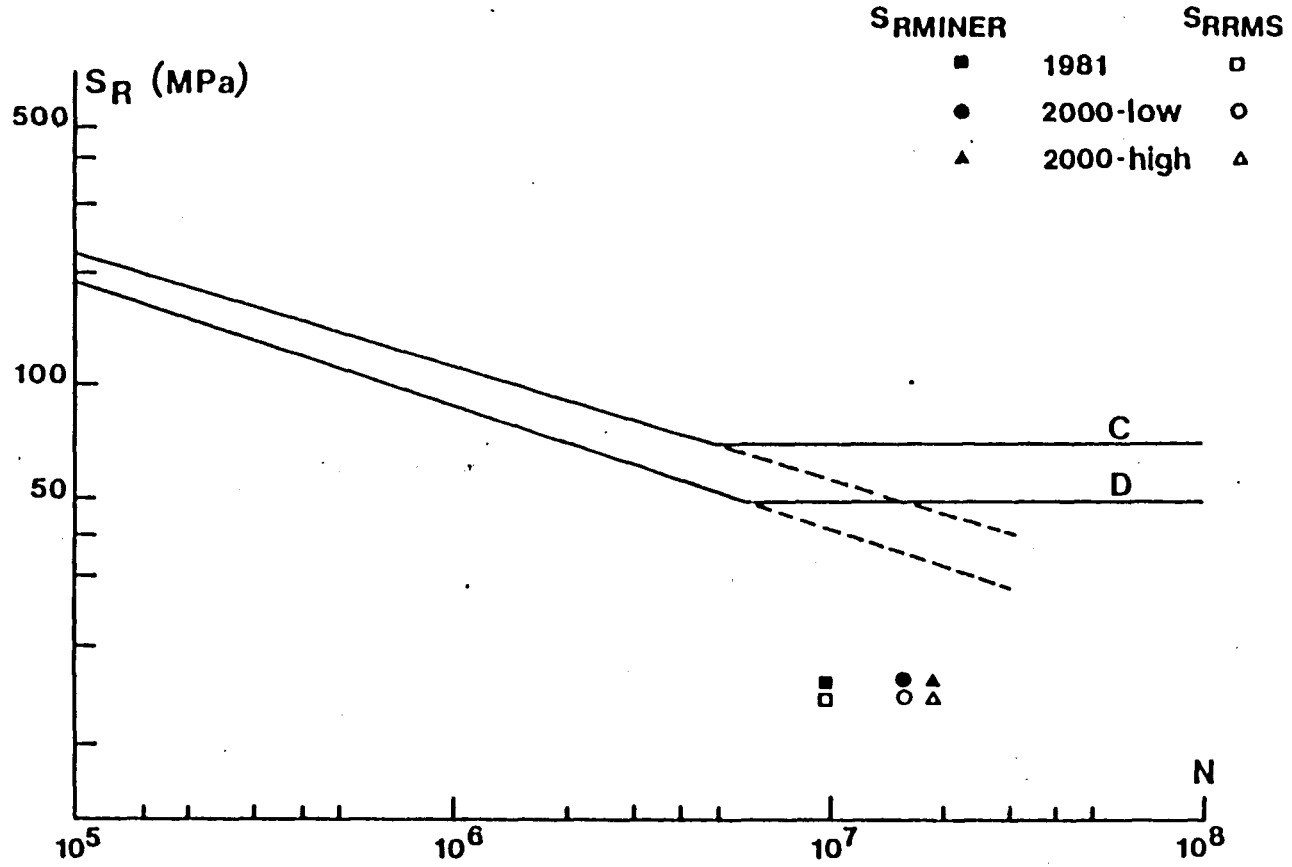

Fig. 37 Fatigue-Life of Critical Hanger

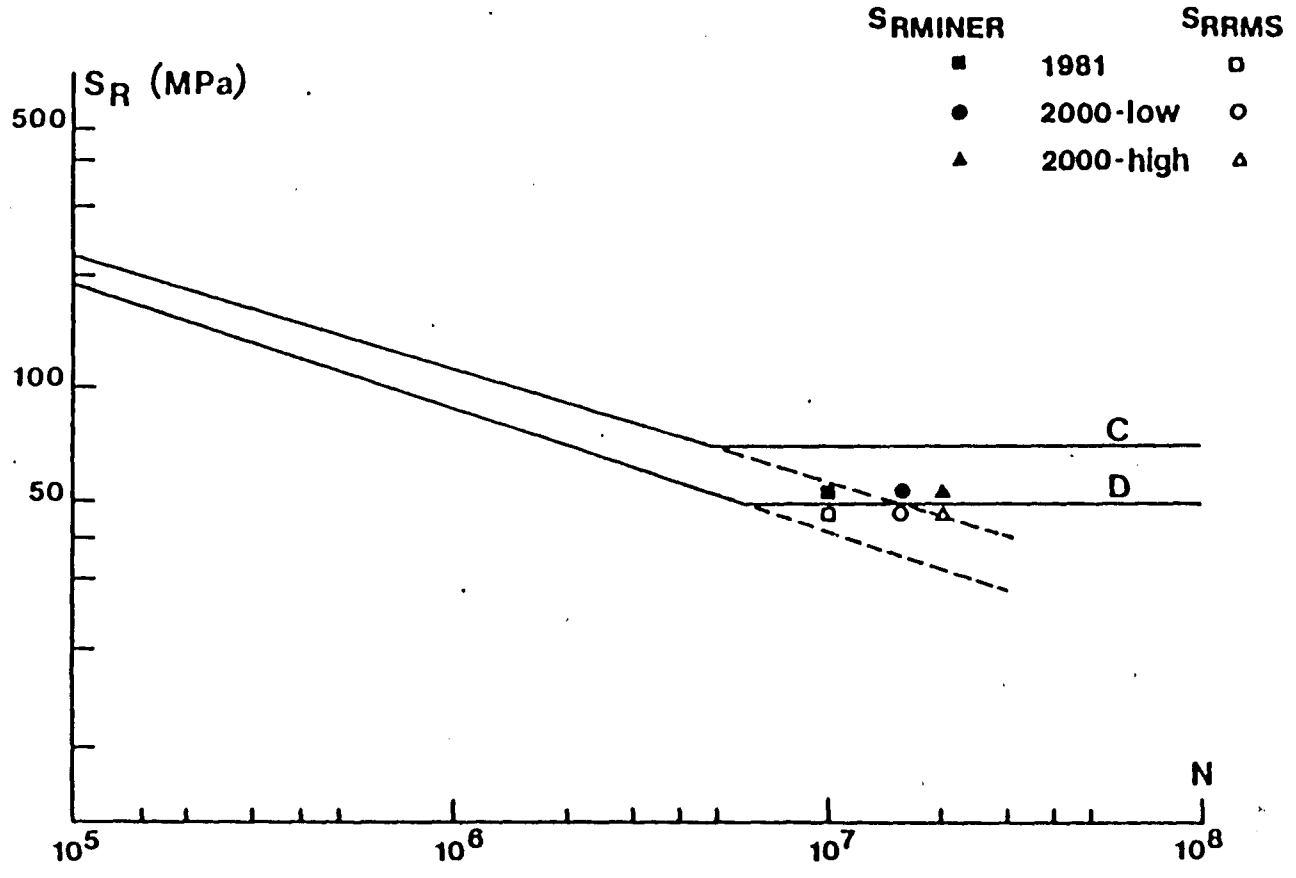

Fig. 38 Fatigue Life of Critical Stringer

APPENDIX A:

COMPUTER PROGRAMS

PROGRAM HISTO

Figure A1 shows a simplified flowchart of program HISTO. The program was written primarily for the data reduction phase of the analysis presented herein. It compiled the data obtained from the analog traces and produced stress histograms for each gage. It also calculated S_{RRMS} and S_{RMINER} for each gage*. All strain range values used as input to the program were in mm. All output was in SI units.

PROGRAM DIMEN AND SUBROUTINE LOADPL

A flowchart of program DIMEN is shown in Fig. A2. The program was written to dynamically allocate storage for subroutine LOADPL.

Figure A3 shows a simplified flowchart of subroutine LOADPL. The subroutine was written to assist in the theoretical analysis of the Blue Nile Bridge. It plotted stress-time curves at gage points to allow for a comparative analysis with the analog traces acquired in the field. It was also used in the fatigue damage estimation of critical members. Stress-time curves were plotted for critical members based on typical train traffic, and these curves were then used to estimate the fatigue life of the total structure.

Table A2 lists the input format for program DIMEN and subroutine LOADPL. All length variables were in inches, and all force variables were in kips. The axle loads for the train under consideration were in long tons (1 long ton = 2240 lbs.). Figure A4 shows a simplified schematic of the input to DIMEN and LOADPL.

---

*Presented in Table A1 is the input format for the program.

TABLE A1: INPUT FOR PROGRAM HISTO

Card No.	Symbol	Format	Description
1	NGAGE	I4	Gage number
	CALVAL	F10.0	Calibration value for gage in mm
	NRANGE	I4	Number of strain ranges to be input
2F*	RANGE	10F8.0	Strain ranges in mm
3	XMIN	F8.0	Threshold strain range value in mm (must be less than or equal to 4 mm)
	NMIN	I5	Number of strain ranges less than the threshold strain range (these range values are not in array RANGE)

*F refers to "and following cards as required"

TABLE A2: INPUT FOR PROGRAM DIMEN AND SUBROUTINE LOADPL

Card No.	Symbol	Format	Description
1	NPTS	I10	Number of points on influence line
	NW	I10	Number of train axles
	TL	F10.0	Train length
	BRL	F10.0	Bridge length
	DX	F10.0	Incremental distance for movement of train
2	NUMMEM	I10	Number of Members
3F*	SPANL	8F10.0	Span lengths of bridge, right to left
4F	WSPACE	8F10.0	Spacing between axles of train, left to right
5F	AXLOAD	8F10.0	Axle loads of train, left to right
6	HDNG	A10	Direction of train (north or south, where north is right to left)
7**	MEMBER	A10	Arbitrary label for member
	AREA	F10.0	Cross-sectional area of member
	SX	F10.0	Section modulus about x-axis for point on cross-section of member under consideration
	SY	F10.0	Section modulus about y-axis for point on cross-section of member under consideration
8F	YINFA	8F10.0	Axial forces in member due to unit loadings
9F	YINFMX	8F10.0	Bending moment about x-axis in member due to unit loadings
10F	YINFMY	8F10.0	Bending moment about y-axis in member due to unit loadings

*F refers to "and following cards as required"
**Cards 7 through 10 are repeated for each member under consideration

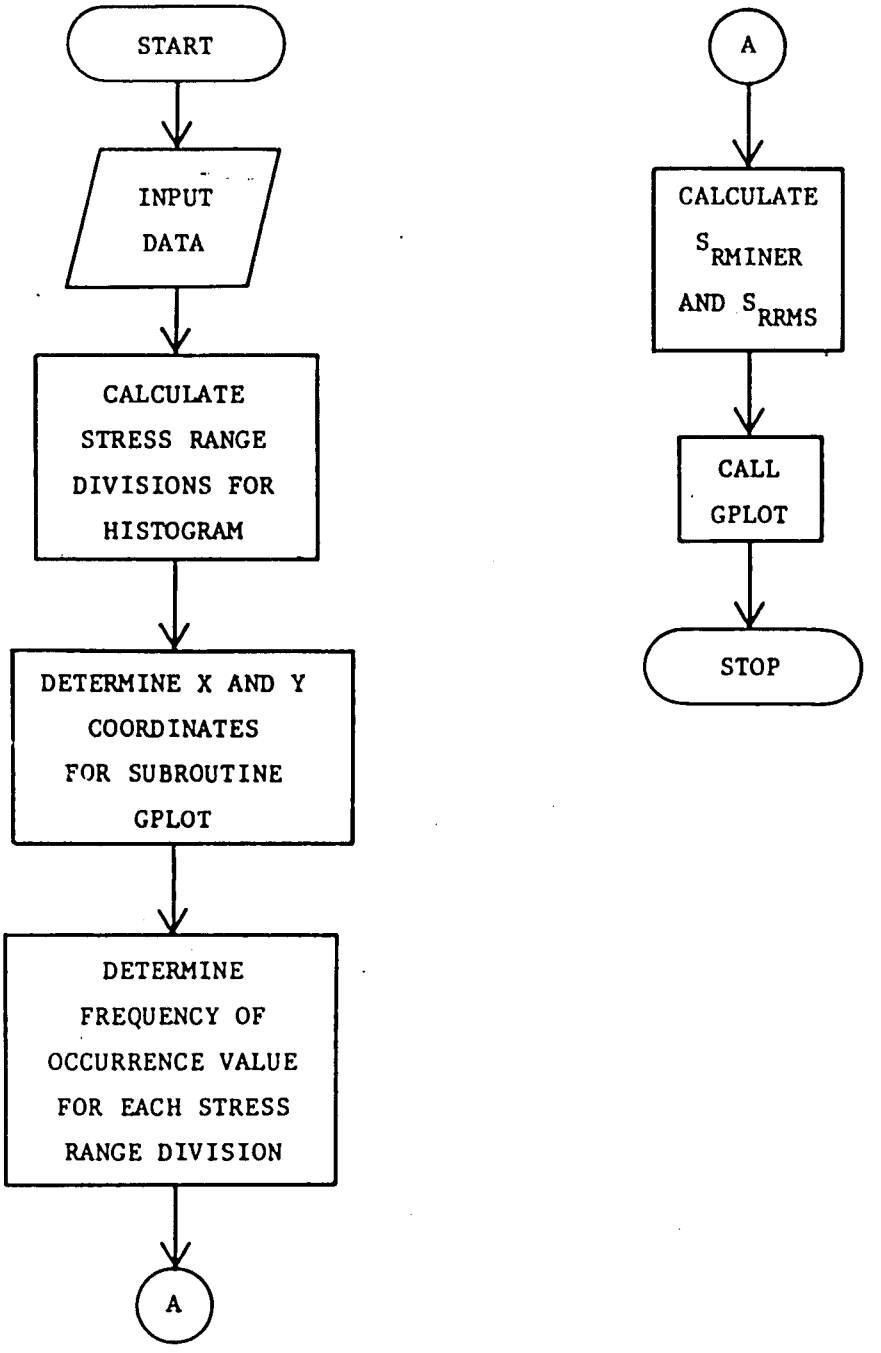

Fig. A1 Flowchart of Program HISTO

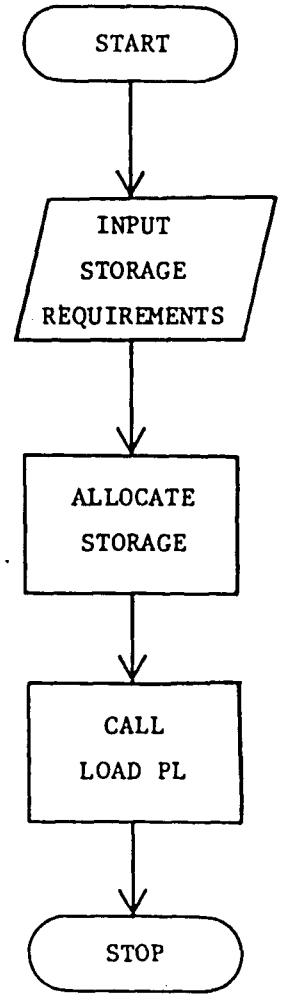

Fig. A2 FlowChart of Program DIMEN

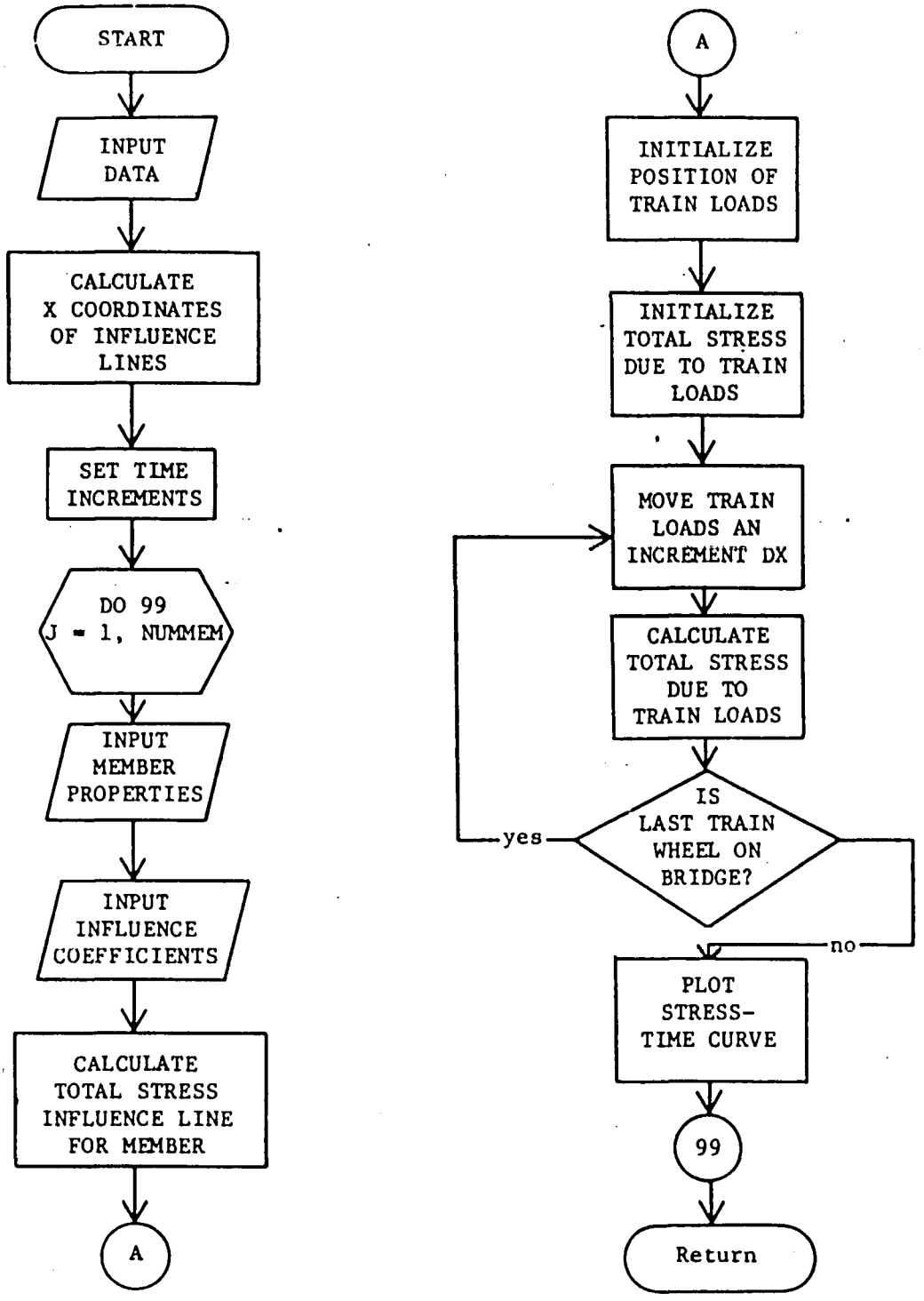

Fig. A3 Flowchart of Subroutine LOADPL

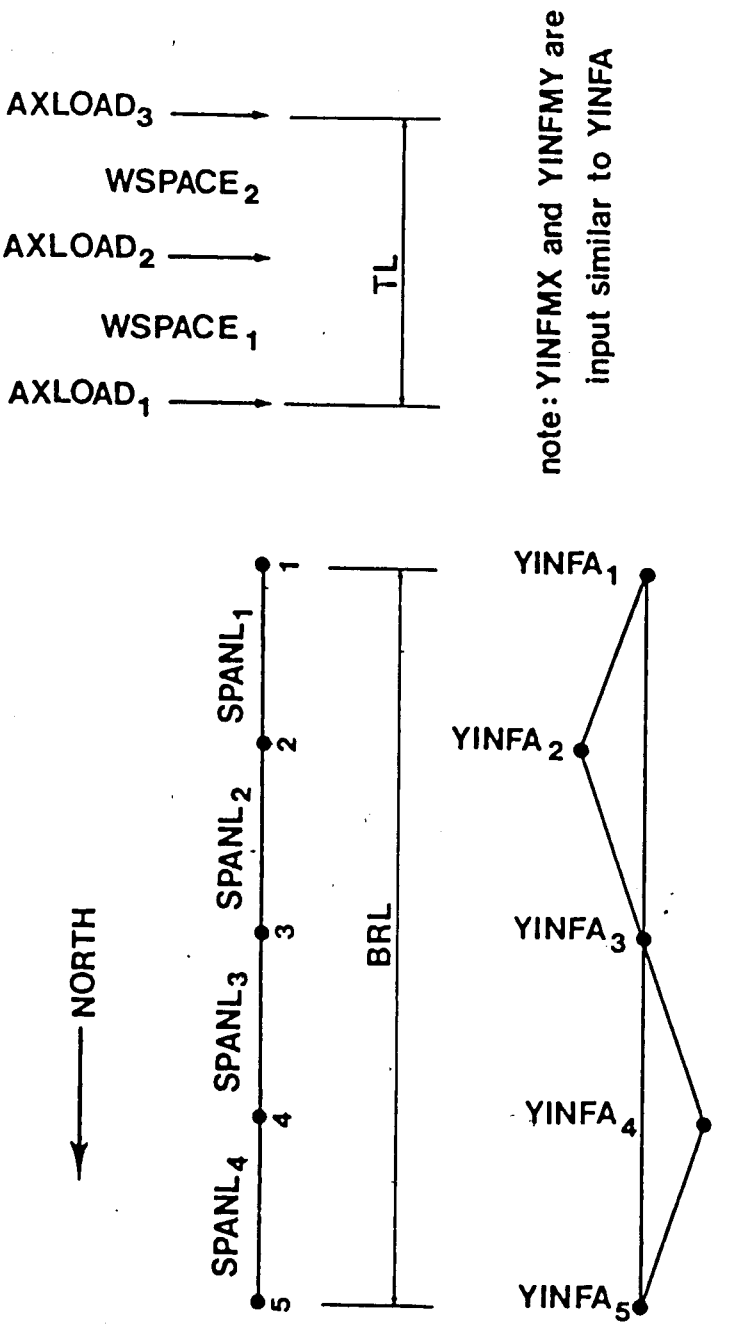

Fig. A4 Schematic of Input for DIMEN and LOADPL

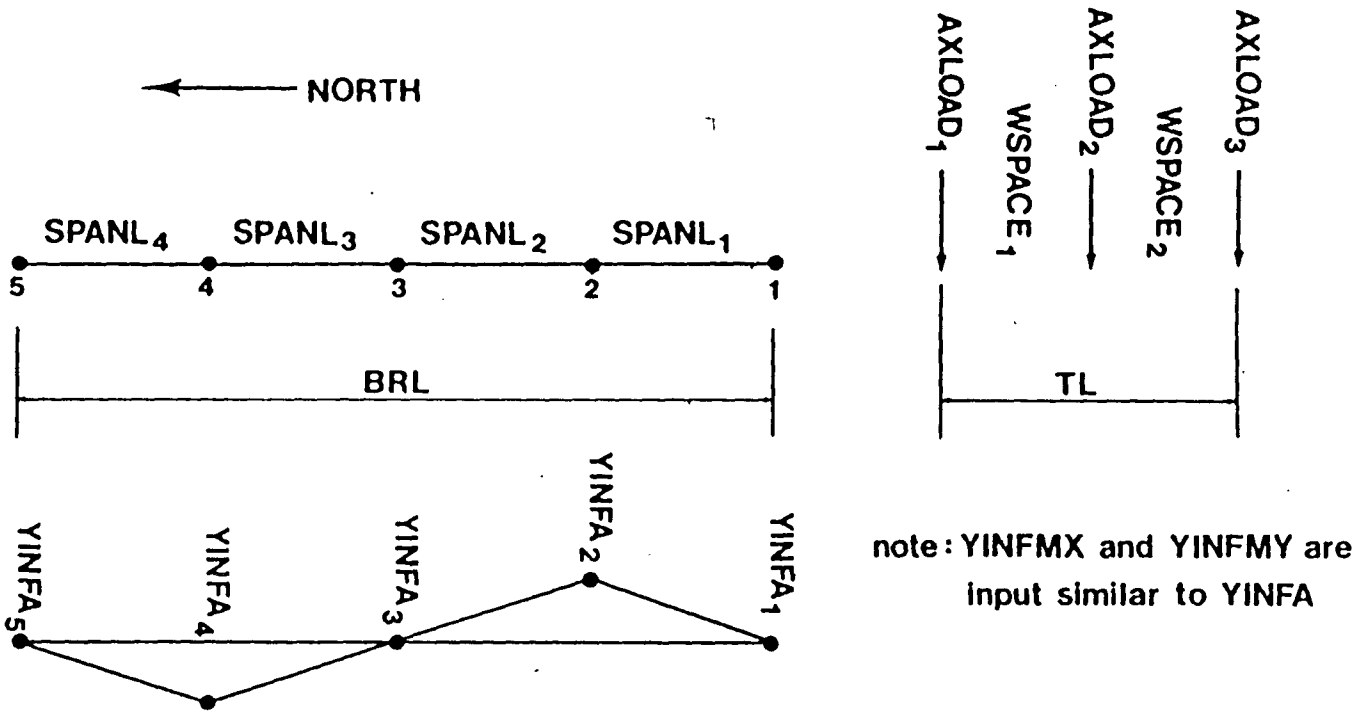

Fig. A4 Schematic of Input for DIMEN and LOADPL

REFERENCES

1. AREA, 1980
   MANUAL FOR RAILWAY ENGINEERING, American Railway Engineering Association, Chicago, Illinois, 1980.

2. Baron, F. and Larson, E. W., 1952
   COMPARATIVE BEHAVIOR OF BOLTED AND RIVETED JOINTS, Technological Institute Research Report C109, Northwestern University, Chicago, Illinois, September 1952.

3. Baron, F. and Larson, E. W., 1952
   THE EFFECT OF GRIP ON THE FATIGUE STRENGTH OF RIVETED AND BOLTED JOINTS, Technological Institute Research Report C110, Northwestern University, Chicago, Illinois, September 1952.

4. Baron, F., Larson, E. W. and Kenworthy, K. J., 1955
   THE EFFECT OF CERTAIN RIVET PATTERNS ON THE FATIGUE AND STATIC STRENGTH OF JOINTS, Report of Research Council on Riveted and Bolted Structural Joints of the Engineering Foundation, New York, New York, February 1955.

5. Bathe, K. J., Wilson, E. L. and Peterson, F. E., 1974
   SAP IV - A STRUCTURAL ANALYSIS PROGRAM FOR STATIC AND DYNAMIC RESPONSE OF LINEAR SYSTEMS, University of California, Berkeley, California, April 1974.

6. Carter, J. W., Lenzen, K. H. and Wyly, L. T., 1954
   FATIGUE IN RIVETED AND BOLTED SINGLE LAP JOINTS, Proceedings of the American Society of Civil Engineers, Vol. 80, Paper No. 469, August 1954.

7. Chu, T. Y., 1962
   THE EFFECT OF BEARING STRESSES ON THE FATIGUE STRENGTH OF A STRUCTURAL JOINT, Report No. 6, Studies in Engineering Mechanics, University of Kansas, May 1962.

8. Coode and Partners, 1960
   REPORT ON THE EXAMINATION OF COAL TRANSPORTERS AND BRIDGES, London, England, July 1960.

9. Engineering Foundation, 1953
THE EFFECT OF GRIP ON THE FATIGUE STRENGTH OF RIVETED AND BOLTED JOINTS, Second Progress Report of the Research Council on Riveted and Bolted Structural Joints of the Engineering Foundation, New York, New York, March 1953.

10. Fisher, J. W., 1977
BRIDGE FATIGUE GUIDE - DESIGN AND DETAILS, American Institute of Steel Construction Booklet T112-11/77, New York City, June 1977.

11. Fisher, J. W. and Daniels, J. H., 1976
AN INVESTIGATION OF THE ESTIMATED FATIGUE IN MEMBERS OF THE 380 FT. MAIN SPAN, FRASER RIVER BRIDGE, American Railway Engineering Association Bulletin 658, June 1976.

12. Lenzen, K. H., 1949
THE EFFECT OF VARIOUS FASTENERS ON THE FATIGUE STRENGTH OF A STRUCTURAL JOINT, American Railway Engineering Association Bulletin 481, Vol. 51, June-July 1949.

13. Lewitt, C. W., Chesson, E. and Munse, W. H., 1959
THE EFFECT OF RIVET BEARING ON THE FATIGUE STRENGTH OF RIVETED JOINTS, Structural Research Series No. 170, Engineering Experiment Station, University of Illinois, Urbana, Illinois, January 1959.

14. Parola, J. F., Chesson, E. and Munse, W. H., 1965
EFFECT OF BEARING PRESSURE ON FATIGUE STRENGTH OF RIVETED CONNECTIONS, Engineering Experiment Station Bulletin 481, University of Illinois, Urbana, Illinois, October 1965.

15. Sandburg, C. H., 1955
INVESTIGATION OF FLOOR BEAM HANGERS IN RAILROAD TRUSSES, Proceedings of the American Society of Civil Engineers, Vol. 81, Paper No. 762, August 1955.

16. Sweeney, R. A. P. and Elkholy, I. A. S., 1980
ESTIMATED FATIGUE DAMAGE ON THE ASSINIBOINE RIVER BRIDGE IN NATTRESS, MANITOBA, Canadian National Railways, Montreal, Quebec, Canada, June 1980.

17. Van Maarschalkerwaart, H. M. C. M., 1981
FATIGUE BEHAVIOR OF RIVETED JOINTS, Netherlands Railway, Utrecht, Netherlands, April 1981.

18. Wilson, W. M. and Thomas, F. P., 1938
FATIGUE TESTS OF RIVETED JOINTS, Engineering Experiment Station Bulletin No. 302, University of Illinois, Urbana, Illinois, 1938.

19. Woodward, H. M. and Fisher, J. W., 1980
PREDICTIONS OF FATIGUE FAILURE IN STEEL BRIDGES, Fritz Engineering Laboratory Report No. 386-12(80), Lehigh University, Bethlehem, Pennsylvania, August 1980.

20. Wyly, L. T. and Scott, M. B., 1955
AN INVESTIGATION OF FATIGUE FAILURES IN STRUCTURAL MEMBERS OF ORE BRIDGES UNDER SERVICE LOADINGS, American Railway Engineering Association Bulletin 524, September 1955.

VITA

Deborah Jean Marcotte was born on October 19, 1956 in Lowell, Massachusetts. She is the second of three children of Alfred G. and Doris T. Marcotte.

The author attended Chelmsford High School in Chelmsford, Massachusetts and graduated in June 1974. She began her undergraduate studies at the College of the Holy Cross in Worcester, Massachusetts. In September 1976, she transferred to the University of Lowell in Lowell, Massachusetts and graduated summa cum laude in May 1980 with the degreee of Bachelor of Science in Civil Engineering.

The author received a fellowship from the American Institute of Steel Construction for graduate study at Lehigh University and began her graduate program in September 1981. As part of her studies, she worked on several projects, including the "Field Studies of Sudan Railroad Bridges."